
Volume 17, Issue 3, 172523 (1-20)

Iranian Journal of Earth Science (IJES)

https://doi.org/10.57647/j.ijes.2025.16801

# Analysis of biomicrofacies in the interpretation of the sedimentary environment of Middle Eocene-Early Miocene deposits in Isa Abad, and Imamzadeh Gahroo (surrounding Chaharmahal and Bakhtiari), Central Zagros

Homa Zulnoorian[1], Kobra Mirbeik Sabzevari[1,*], Borzu Asgari Pirbalouti[2], Seyed Vahid Shahrokhi[1], Siamak Baharvand[1]

[1]*Department of Geology, Khorramabad Branch, Islamic Azad University, Khorramabad, Iran.*
[2]*Department of Petroleum Engineering, Masjed Soleiman Branch, Islamic Azad University, Masjed Soleiman, Iran.*

[*]**Corresponding author:** k_mirbeik_s@yahoo.com

**Original Research**

Received:
11 February 2024
Revised:
1 April 2024
Accepted:
20 June 2024
Published online:
10 July 2025



**Abstract:**

The middle Eocene-early Miocene deposits have been sampled in the stratigraphic sections of Isa Abad and Imamzadeh Gahroo, Chaharmahal, and Bakhtiari, to determine the sedimentary environment based on microfacies analysis. Nine carbonate microfacies have been identified based on microscopic studies, where the inner, middle, and outer ramps are located in three facies belts. In the inner ramp, the MF1 and MF2 microfacies indicate an enclosed lagoon considering the presence of perforate benthic foraminifera in huge numbers, corallinaceae algae, ostracods, gastropods, and peloid. Also, the MF3 and MF4 microfacies indicate a lagoon with free water rotation and the absence of a continuous reef due to the simultaneous presence of perforate and imperforate benthic foraminifera. In Shoal (Microfacies MF5), bioclasts and ooids are the major grains, along with peloids, intraclasts, corallinaceae algae, echinoids, bryozoans, and corals. In the middle ramp (microfacies MF6 to MF8), considering the presence of large hyaline species (*Lepidocyclina*, *Miogypsina*, and *Nummulitidae*), the stretched shape of these species, the large size of the allochems, their association with corallinaceae algae, the diversity and abundance of species, the small presence of planktonic and porcelaneus species are evident. In these sections, the outer ramp (Microfacies MF9) can be identified by the presence of planktonic species, the small number of benthic species, and the abundance of the matrix. Due to the gradual conversion of microfacies into each other, the lack of abundance of shoaling ooid and peloid microfacies, and the absence of turbidities and collapse breccia's, the sedimentary environment of these deposits can be attributed to a homoclinal ramp.

**Keywords:** Eocene; Miocene; Microfacies; Sedimentary environment; Central Tethys

## 1. Introduction

The Paleocene to Eocene Jahrom Formation hosts, together with the Oligo-Miocene Asmari Formation, the most important reservoir rocks in the Near East. However, these sequences are still poorly explored in their outcrops, especially in the central Zagros.

In this center, part of Tethyan, the shallow-water carbonates of the Eocene Jahrom Formation and the mixed, shallow-water carbonates and sandstones of the Oligocene-Miocene Asmari Formation are spread. Paleocene and, in particular, the Eocene platforms first developed around the margins of this Tethyan basin, progressing towards the center (Van Buchem et al., 2010). The Asmari carbonates are in the margins of an intrashelf basin in the central segment of the Tethyan seaway in the Zagros foreland basin (Van Buchem et al., 2010) and indicated the last marine transgression of the Neo-Tethys Ocean (Stocklin, 1968; Berberian and King, 1981; Alavi, 1994, 2004; Heydari, 2008).

The shallow marine (carbonate platform) deposits are well-developed into two belts along the Tethyan system (Scheibner and Speijer, 2008; Hontzsch et al., 2013; Martin-Martin et al., 2020, 2021; Jehangir Khan et al., 2021; Tosquella et al., 2022). A northern belt (middle latitudes: about 40°N) was located from the Pyrenees to the Tibetan region comprising the Alpine, Adriatic, Apennine, Carpathian, Great Caucasus, Hellenian, Anatolian, and Indian systems), while the southern belt (mostly below 25°N) extended from Morocco to Oman, including Tunisia, Libya, Egypt, and Arabia. In the Middle East, a thick (hundreds of meters) and extensive (plate-scale) Eocene to Miocene carbonate sedimentary record occurs and is rich in larger foraminifera (Arjmandzadeh et al., 2020; Tosquella et al., 2022). Due to the high diversification and extinction rates of the larger foraminiferal genera and species throughout the Eocene and Oligocene, these organisms are key biostratigraphic markers for this period (Cahuzac and Poignant, 1997; Serra-Kiel et al., 1998; Bassi et al., 2007; Boukhary et al., 2010; Habibi, 2016a, 2016b, 2017; Ferràndez-Caadell and Bover-Arnal, 2017).

In recent years, many studies have been focused on microfacies and sedimentary environments of the Jahrom and Asmari formations in the Zagros Basin. Soltani Najafabadi et al. (2018) studied microfacies and the sedimentary environment of the Jahrom Formation in the Saldoran and Dasht-e-Zari sections (high Zagros). Parvaneh Nejad Shirazi et al. (2020) researched the sedimentary environment of the Jahrom Formation in the northwest of Shiraz (Chellehgah Sepidan). The sedimentary environment and sequence stratigraphy of the Jahrom Formation with a view on paleoecology in the interior Fars were investigated by Yazdanpanah et al. (2022).

Van Buchem et al. (2010) studied the depositional sequences of Oligo-Miocene deposits in the Dezful Embayment Zone. Depositional architecture and sequence stratigraphy of the Oligo–Miocene Asmari platform in the southeastern Izeh Zone were investigated by Shabafrooz et al. (2015). Allahkarampour Dill et al. (2018) studied Oligo-Miocene carbonate platform evolution in the northern margin of the Asmari intra-shelf basin. Naseri-Karimvand et al. (2019) studied the depositional environment and sequence stratigraphy of the Oligo-Miocene deposits north and east of Dehdasht, Izeh Zone. Abyat et al. (2019) researched microfacies and the depositional environment of the Asmari Formation in the Zeloi oil field. Joudaki et al. (2020) studied the regional facies analysis and depositional environments of the Oligocene and Lower Miocene deposits in the Zagros Basin. Petrography, sedimentary environment, and reservoir potential assessment of the Asmari Formation in the KilorKarim oil field (Dezful Embayment) were investigated by Ahmadi et al. (2022); Mirzaee Mahmoodabadi (2023); Saadat et al. (2023) studied the sedimentation-diagenesis history of Paleocene-Miocene succession (Jahrom and Asmari formations) in the southern part of Dezful Embayment.

So far, the microfacies and sedimentary environment of the Jahrom-Asmari Fms in the Isa Abad and Imamzadeh Gahroo sections have not been studied. In this study, an attempt has been made to investigate these microfacies and present a sedimentary model for the Middle Eocene to Early Miocene deposits in the Isa Abad and Imamzadeh Gahroo in the Central Zagros (Fig. 1).

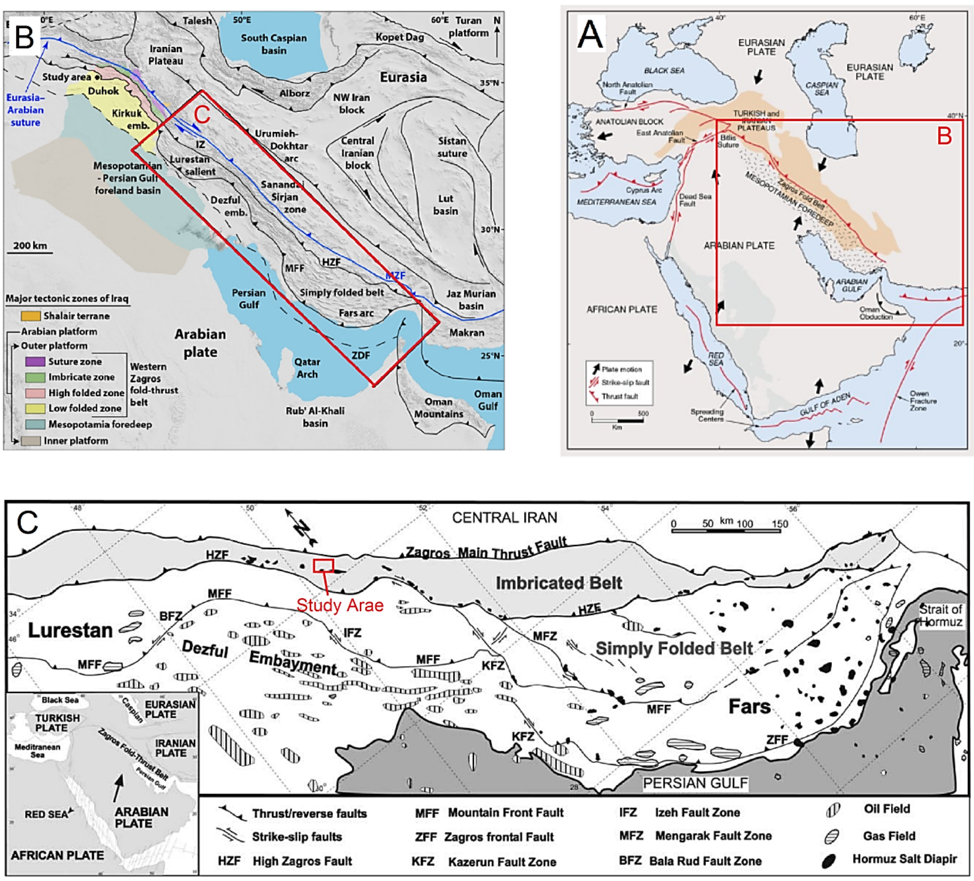


**Figure 1.** (A) Tectonic Units of the Middle East (**Saber et al. 2000?**), Gulf PetroLink, https://exhibits.library.cornell.edu/barazangi-map-collection/catalog/60-2789. (B) Major tectonic zones of Iran (Doski and Mc Clay, 2022) (C) Structural setting of the Zagros Fold– Thrust-Belt showing the major fault zone (Sepehr and Cosgrove, 2004) and study area.

## 2. Study area

The studied sections are located in Chaharmahal and Bakhtiari province. Isa Abad section is 39 km west of Shahr-e kord. The geographical coordinates of this section are 32° 13′ 07″ N and 50° 32′ 28″ E (Fig. 2). To access this stratigraphic section, crossing 5 km on an asphalt road from Farsan, you arrive in Gojan, and then driving about 5 km to the southwest, you can access this stratigraphic section. The Imamzadeh Gahroo section is located 36 km south of Shahr-e kord and 8 km southeast of Shalamzar. The geographical coordinates of this section are 32° 10′ 31″ N and 50° 52′ 00″ E (Fig. 1). To arrive at this section, the asphalt road from Shahr-e kord to Shalamzar can be used. Crossing Shalamzar, after driving 8 km on an asphalt road toward the village of Gahroo, you will arrive at the section.

## 3. Methodology

Sampling is systematically carried out in studied sections in 1 to 1.5 m intervals. In this study, 80 thin sections of Imamzadeh Gahroo and 68 thin sections of Isa Abad have been studied. Then the prepared microscopic sections were examined with a polarizing microscope. The carbonate rocks were named using Embry and Klovan (1971) and Dunham (1962) methods. Visual comparison charts were used for the estimation of major and minor components. In the present study, the microfacies and sedimentary environment of this formation were determined by combining and comparing Wilson (1975) and Flügel (2010) methods.

## 4. Stratigraphy

Middle Eocene-Early Miocene deposits in the studied sections include Jahrom and Asmari formations. Jahrom Formation includes Paleocene to Eocene formations of Zagros Basin. The type section of this formation is on the northern flank of Jahrom Mount, which includes 467.5 meters of dolomite and dolomitic limestone. In the type section, this formation is overlain by the Sachun Formation with a compatible boundary and has a continuous and progressive boundary with the Asmari Formation at the top (Motiei, 1993). Asmari Formation consists of carbonate rocks of Oligocene to Miocene age that have been deposited on a carbonate platform throughout the Zagros Basin and its most intact sequence has been seen in the Dezful Embayment (Motiei, 1993). In terms of lithostratigraphy, sedimentary environments, and age characteristics, changes are seen in this formation in other regions of Zagros.

Richardson (1924) measured the sample section of this formation in Asmari Mount (Tang Goltorsh) and considered it comparable to Khamir limestone in the Fars region. Lees (1933) revised previous ideas, and in fact, he was the founder of today's attitudes about the Asmari Formation. He has considered the basic anhydride of Asmari Formation as a part of this formation. Thomas (1948) has conducted relatively comprehensive studies on the Asmari Formation. While confirming Lees (1933) works, he classified the progressive layers within the Asmari Formation and considered the age of this formation from Oligocene to Burdigalin. He also considered the basic anhydride of this formation in the Asmari Mount as equivalent to the *Eulepidina* fossil strata in the Asmari of Gachsaran field. James and Wynd (1965) summarized the previously described results of the Asmari Formation and published a new definition of the Asmari Formation. These researchers considered the Jarib and Euphrates formations from Iraq and Khamir limestone from the Fars region to be equivalent to Asmari Formation and introduced Ahwaz sandstone sediments and Kalhor evaporative sediments as their members.

The studied sections related to the Middle Eocene to the Early Miocene sediments of the Jahrom and the Asmari formations. The Jahrom Formation is overlain by the Pabedeh Formation with a continuous border. The boundary between

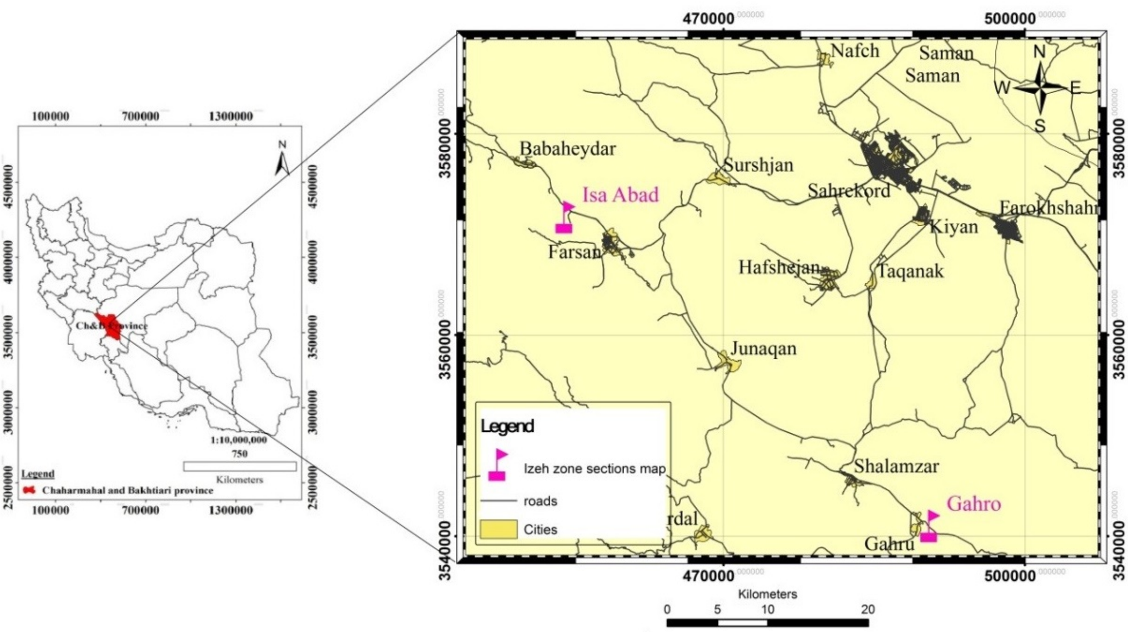


**Figure 2.** Ways of access to the stratigraphic sections of Isa Abad and Gahroo in the study area.

Jahrom and Asmari formations is not recognizable in the field, but biostratigraphic data show that this boundary is continuous, so the last biozone of Jahrom Formation (*Nummulites fabiani- Chapmanina* assemblage zone), from the Late Eocene, is overlain by the first biozone of Asmari Formation (*Nummulites vascus* assemblage zone -*Nummulites fichteli*), from the Rupelian. This indicates that the boundary between these two formations is continuous in both sections. The upper boundary of the Asmari Formation is discontinuously covered with evaporative sediments of the Gachsaran Formation (Figs. 3 (a) & (b)). The Middle Eocene to The Early Miocene sediments in the Isa Abad section with an actual thickness of 151.5 m include limestones and fossil-filled and nodular sandstones. This bottom-up stratigraphic column consists of 6 sedimentary units as follows: The first sedimentary unit consists of middle-layer gray limestones, the thickness of which is 6.5 meters. The second sedimentary unit is composed of thick sandstone limestones of cream color. The thickness of this unit is 9 meters. The third sedimentary unit consists of alternating limestone, sandstone nodular sand limestones, and white cherts with a thickness of 31 meters. The fourth sedimentary unit is composed of fossilized gray mass limestone 21 m thick (Fig. 3 (c)). The fifth sedimentary unit consists of 49 m of nodular gray mass limestones. The sixth sedimentary unit consists of thick-layered limestones and cream-colored masses with weathered and crushed surfaces with a thickness of 35 meters. Units 1 to 3 indicate the Jahrom Formation related to the Middle to Late Eocene and units 4 to 6 indicate the Asmari Formation related to the Rupelian to the Burdigalian.

In the Imamzadeh Gahroo section, the Middle Eocene to Early Miocene sediments are 179 meters thick and consist of 8 sedimentary units. The first unit with a thickness of 14 meters is composed of fossil gray limestone and the second unit is composed of 16 meters of cream-colored limestone. The third unit consists of 18-meter-thick gray microcrystalline mass limestones. This unit contains many fossils. The fourth unit consists of a thick-layered limestone to a rocking cream-colored mass with a thickness of 23 meters. Limestone is a hard and dense cream-colored mass with a thickness of 16 meters, which forms the fifth sedimentary unit. The sixth sedimentary unit consists of thick-layered fossil-containing gray limestones with a thickness of 19 meters. The seventh unit is 25 m thick and consists of a purple-colored nodular limestone mass (Fig. 3 (d)). The eighth sedimentary unit is composed of dense cream-to-white mass limestone with a thickness of 48 meters. Units 1 to 6 indicate the Jahrom Formation from the Middle to Late Eocene and units 7 and 8 indicate the Asmari Formation from the Rupelian to the Burdigalian.

Biostratigraphy studies of the Gahroo and Isa Abad sections in Central Zagros led to the identification of 7 biozones in the Isa Abad section and eight biozones in the Gahroo section (Table 1). In the sediments of Jahrom Formation in Isa Abad section were identified *Dictyoconus – Coskinolina–Orbitolites complanatus* assemblage subzone (Middle Eocene), *Nummulites-Alveolina* assemblage subzone (Middle Miocene), *Chapmanina- Baculogypsinoides* assemblage zone (Late Miocene) as well as, in the Gahroo section were identified four biozones in this formation that include: the *Linderina* subzone (Middle Miocene), *Dicty-*

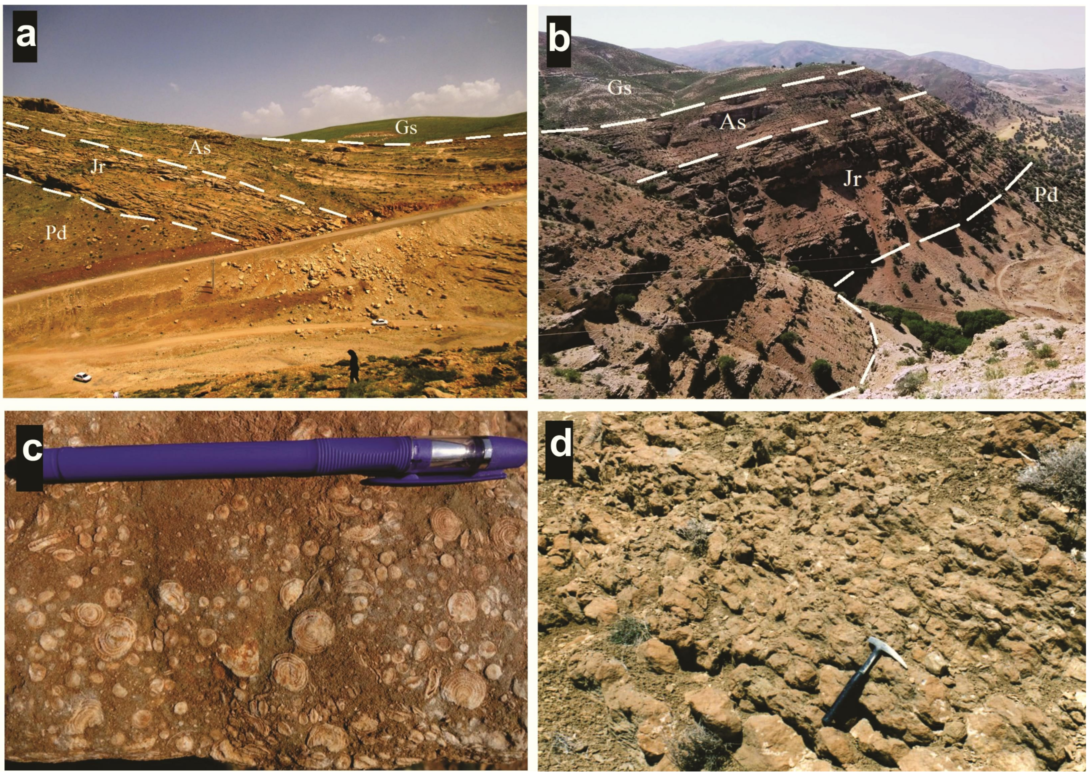


**Figure 3.** (a) Boundary of Pabedeh, Jahrom, Asmari, and Gachsaran formations in the Isa Abad section, view toward the north. (b) Boundary of Pabedeh, Jahrom, Asmari and Gachsaran formations in the Imamzadeh Gahroo section, view toward the northwest. (c) Gray fossil-filled limestone of the unit 4, Isa Abad section. (d) Nodular limestone mass in unit 7 in the Gahroo section.

**Table 1.** Correlation chart of the defined biozones with **Laursen2009<empty citation>** and James and Wynd (1965) biozonation.

| epoch | age | Wynd1965<empty citation> | | | | Laursen2009<empty citation> | | this study: Eisa Abad | this study: Gahro |
|---|---|---|---|---|---|---|---|---|---|
| Miocene | Burdigalian | *Borelis melocurdica (No.61)* | | | | *Borelis melocurdica- Borelis melo melo* | | *Borelis melocurdica- Borelis melo melo* | *Borelis melocurdica- Borelis melo melo* |
| Miocene | Aquitanian | *Austrotrillina howchini- Peneroplis evolutus (No.59)* | | | | *Miogypsina- Elphidium sp. 14- Peneroplis* | Indeterminate | Indeterminate zone | Indeterminate zone |
| Oligocene | Chattian | *Archaias operculinoformis (No.58)* | *Nummulites intermedius- Nummulites vascus (No.57)* | *Lepidocyclina - Operculina - Ditrupa (No. 56)* | *Globigerina spp. (No.55)* | *Archaias asmaricus- Archaias hensoni- Siogypsinoides* | *Lepidocyclina – Operculina– Ditrupa* | *Lepidocyclina Operculina Ditrupa* | *Archaias asmaricus- Archaias hensoni Miogypsinoides* |
| Oligocene | Rupelian | | | | | *Nummulites vascus- Nummulites fichteli* | *Globogerina- Turborotalia cerroazulensis Hantkenina* | *Nummulites vascus – Nummulites fichteli* | *Nummulites vascus – Nummulites fichteli* |
| Eocene | upper | *Chapmanina – Pellatispira – Baculogypsinoides (No.53)* | | | | | | *Chapmanina- Baculogypsinoides* | *Nummulites fabiani* |
| Eocene | middle | *Nummulites - Alveolina (No. 51)* | | | | | | *Nummulites - Alveolina* | *Nummulites - Alveolina* |
| Eocene | middle | *Dictyoconus – Coskinolina – Orbitolites complanatus (No.50)* | | | | | | *Dictyoconus – Coskinolina – Orbitolites complanatus* | *Dictyoconus – Coskinolina – Orbitolites complanatus* |
| Eocene | middle | *Linderina subzone (No.49)* | | | | | | | *Linderina subzone* |
| Eocene | middle | *Somalina subzone (No.48)* | | | | | | | |

*oconus– Coskinolina– Orbitolites complanatus* assemblage subzone (Middle Miocene), *Nummulites - Alveolina* assemblage subzone (Middle Miocene) *Nummulites Fabiani* taxon range zone (Last Eocene). According to identified biozones, Jahrom Formation's age in these sections is middle Eocene-late Miocene. In the sediments of the Asmari Formation in the Isa, Abad section identified four biozones that consist of *Nummulites vascus-Nummulites fichteli* assemblage zone (Rupelian), *Lepidocyclina-Operculina- Ditrupa* assemblage zone (Chattian), Indeterminate zone (Aquitanian), *Borelis melocurdica- Borelis melo melo* assemblage zone (Burdigalian). Also, the Gahroo section recognized four biozones that consist: *Nummulites vascus-Nummulites fichteli* assemblage zone (Rupelian), *Archaias asmaricus-Archaias hensoni- Miogypsinoides complanatus* assemblage zone (Chattian), Indeterminate zone (Aquitanian), *Borelis melocurdica- Borelis melo melo* assemblage zone (Burdigalian). Accordingly, in the studied sections, the age of the Asmari Formation is Rupelian to Burdigalian (Zulnoorian et al., 2023).

## 5. Results

### 5.1 Sedimentary microfacies

The microfacies identified in the studied sections seaward from the shore are as follows (Figs. 4 and 5, Table 2):

**MF1: Bioclastic Miliolidae wackestone-packstone**

The foraminifera identified in this microfacies are Miliolidae, *Triloculina trigonula, Quinqueloculina* sp., *Pyrgo* sp., *Austrotrillina asmariensis* (Overall 30 – 40%). Red algae (10 – 15%), ostracoda (5 – 10%), gastropod (5%) and peloid (5%) are also seen in this microfacies. This microfacies has a lot of micrites and supporting muds. Its

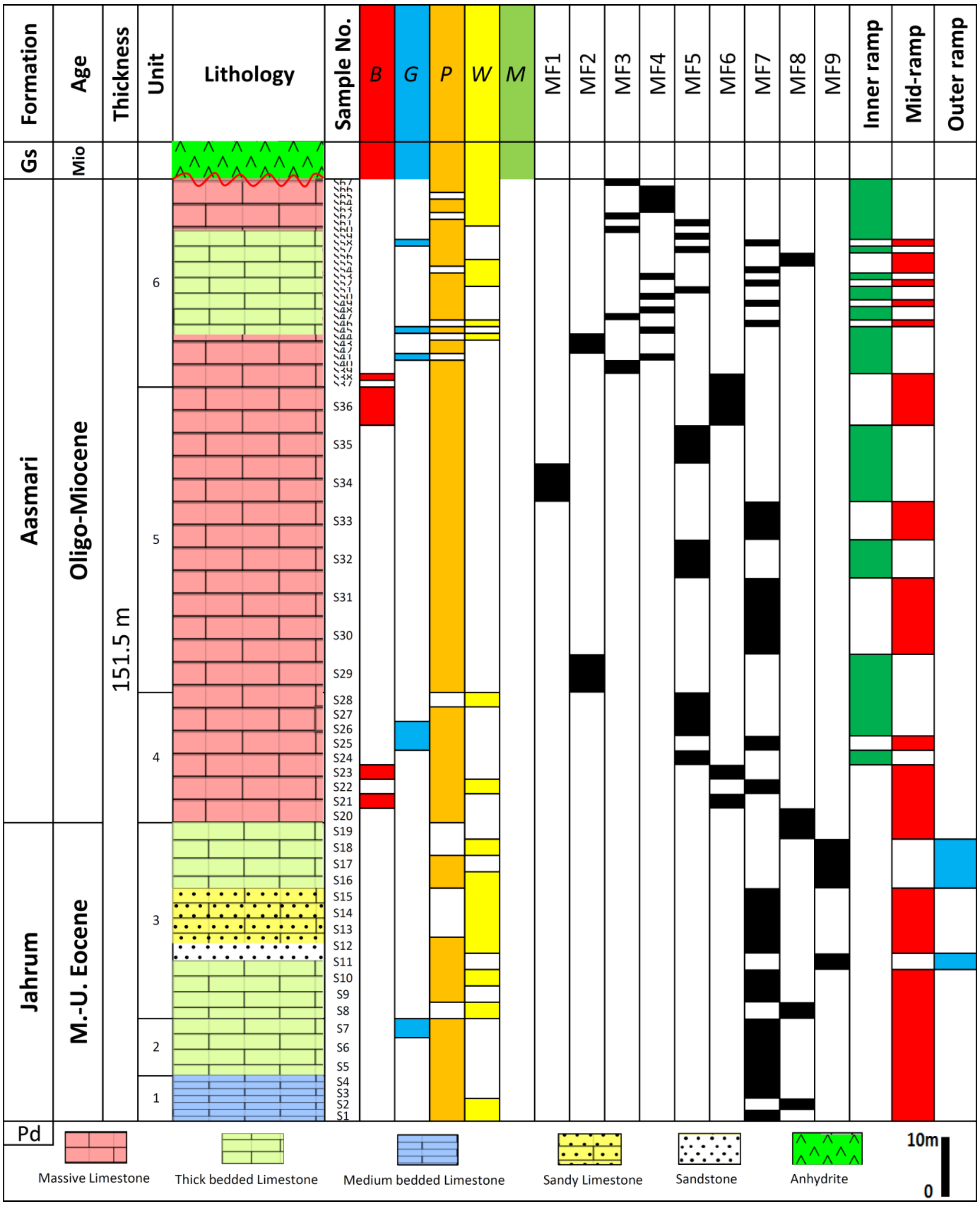


**Figure 4.** Identified microfacies and sedimentary environment of Middle Eocene to Early Miocene in Isa Abad stratigraphic section.

grains are at the lutite size.

Interpretation: As can be seen, benthic foraminifera with porcelaneous walls from the family Miliolidae are the main components. Miliolidae represents an enclosed lagoon (Geel, 2000); Hallock and Glenn1986. The presence of foraminifera with porcelaneous shell in this microfacies indicates an environment with relatively high salinity (Geel, 2000).

**MF2: Imperforate foraminifera wackestone-packstone**

This microfacies consists of imperforated foraminifera. The most important foraminifera identified are: *Borelis inflate, Borelis pygmaea, Borelis* sp., *Archaias* sp., *Alveolina aragonensis, Alveolina ellipsoidalis* (Overall 15 – 20%), *Triloculina trigonula, Quinqueloculina* sp., and Miliolidae (Overall 10 – 15%). In addition, peloids (5 – 10%), bivalvia (5 – 10%) and red algae (5 – 10%) are also seen. The microfacies MF2 has large amounts of micrite and it is classified as mud-supported facies. Similar to the previous microfacies (MF1), the grains are about the size of a lutite.

Interpretation: The presence of perforate foraminifera, *miliolids*, and micrites indicates that the microfacies has been formed in a shallow and low-energy environment. According to the studies Van Buchem et al. (2010), the identified species belong to the lagoon environment of the Asmari Formation. Imperforate foraminifera indicate limited water circulation and hypersaline conditions (**Hallock1986**; Wilson, 1975; Geel, 2000; Romero et al., 2002; Flügel, 2010). As a result, this microfacies is formed in an enclosed lagoon.

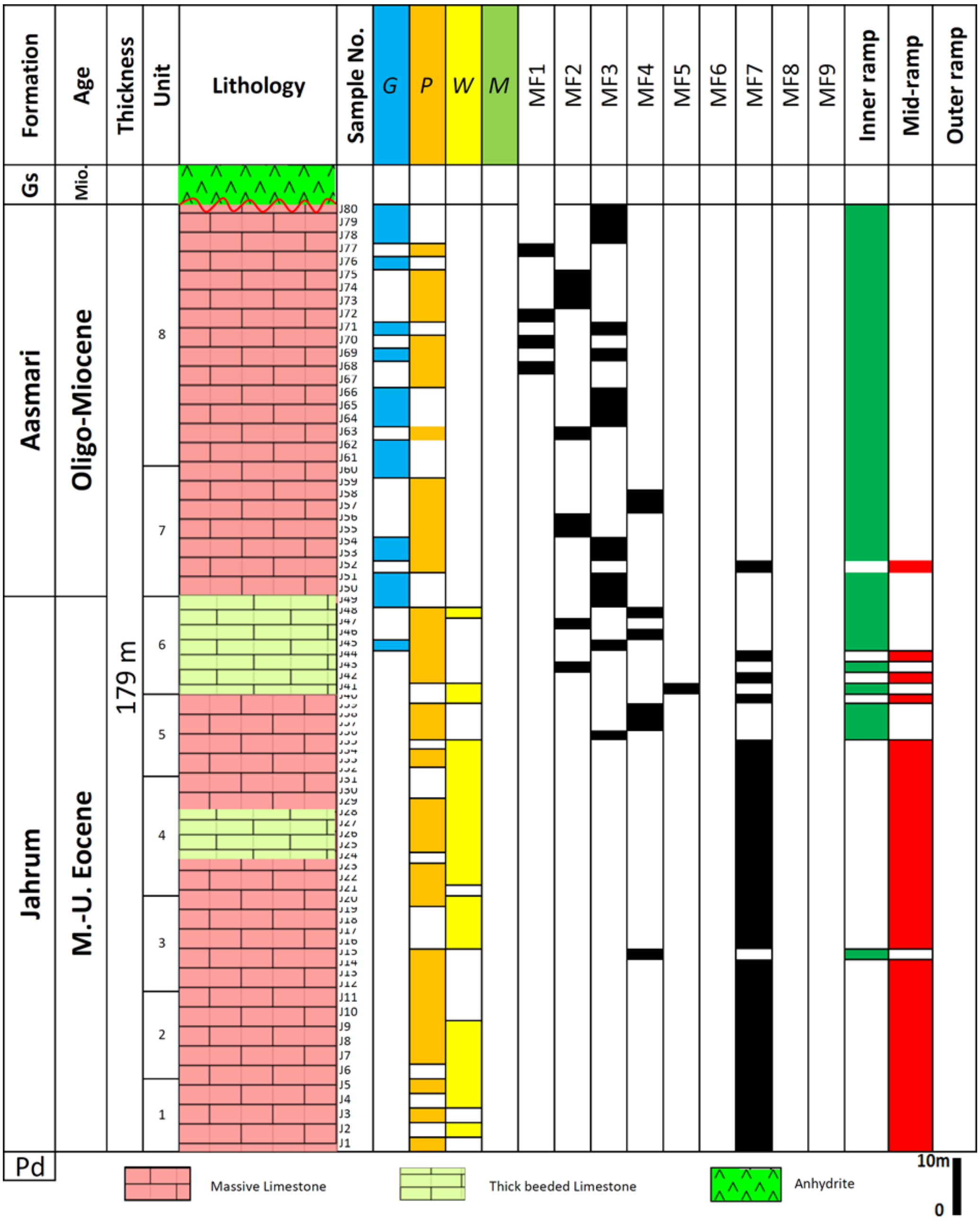


**Figure 5.** Identified microfacies and sedimentary environment of Middle Eocene to Early Miocene in Gahroo stratigraphic section.

**Table 2.** Characteristics and interpretations of facies defined in the Jahrom-Asmari formations in studied section.

| **icrofaceis** | **components** | | **facies belt** |
|---|---|---|---|
| | **skelatal** | **non-skelatal** | |
| MF1: Bioclastic Miliolidae wackestone-packstone | Miliolidae, *Triloculina trigonula, Quinqueloculina* sp., *Pyrgo* sp., Austrotrillina asmariensis, Red algae ostracoda and gastropod | peloid | Inner Ramp |
| MF2: Imperforate foraminifera wackestone-packstone | Imperforate foraminifera (*Borelis inflate, Borelis pygmaea, Borelis* sp., *Archaias* sp., *Alveolina aragonensis, Alveolina ellipsoidalis, Triloculina trigonula*) bivalvia, red algae | peloid | |
| MF3-Bioclastic imperforate foraminifera corallinaceae packstone-grainstone | Coralineceae algae, *Archaias* sp., *Alveolina* sp., *Borelis pygmaea, Quinqueloculina* sp., *Pyrgo* sp., bivalvia, bryozoans | peloid | |
| MF4- Bioclastic perforate and imperforate foraminifera packstone-grainstone | *Archaias* sp., *Lepidocyclina* sp., *Rotalia vinoti, Operculina complanata, Borelis* sp., *Pyrgo* sp., *Alveolina* sp., coralline algae, bivalves, echinoid spines | peloid | |
| MF5- Bioclast ooid packstone-grainstone | *Operculina complanata, Archaias* sp., *Lepidocyclina* sp., *Borelis* sp., miliolids), algae, echinoids, bryozoans, corals | Ooid, intraclasts , prloid | |
| MF6-Coralline red algae–coral rudstone-floatstone | corallinaceae algae, corals, *Borelis inflata, Nephrolepidina praemarginata, Spiroclypeus blanckenhorni, Rotalia* sp., *Amphistegina* sp., *Lepidocyclina* sp., bryozoans. | Intraclasts | Middle Ramp |
| MF7- Large benthic foraminifera bioclastic wackestone-packstone | *Eulepidina dilatata, Eulepidin* sp., *Lepidocyclina* sp., *Operculina complanata, Operculina* sp., *Rotalia* sp., corallinaceae algae, echinoids, and bryozoans | intraclasts | |
| MF8- Bioclastic Lepidocyclinid-Nummulitid wackestone-packstone | *Nummulites vascus Lepidocyclina* sp. *Operculina complanata, Nephrolepidina* sp., *Nephrolepidina tournoueri, Heterostegina assilinoides, Eulepidina* sp., corallinaceae algae, bryozoans, echinoids, *Globigerina* sp. | - | |
| MF9- Planktonic foraminifera wackestone–packstone | *Globorotalia* sp., *Globigerina* sp., echinoids, bivalvia fragments, benthic foraminifera | - | Outer Ramp |

**MF3: Bioclastic imperforate foraminifera corallinaceae packstone-grainston**

Coralineceae algae (30 – 40%) and imperforated foraminifera (15 – 20%) are the main grains of this microfacies. Among the identified imperforated foraminifera, we can mention *Archaias* sp., *Alveolina* sp., *Borelis pygmaea, Quinqueloculina* sp., *Pyrgo* sp. In addition, bivalvia (5%) and bryozoans (5%) are also found in this microfacies. The MF3 microfacies a grain-supported and contain a lot of sparite. Its grains are the size of an arenite.

Interpretation: Red algae in the Oligo-Miocene sedimentary basin have been reported from inner and middle ramp sediments (Van Buchem et al., 2010; Joudaki et al., 2020). The presence of porous benthic foraminifera indicates that in these incisions, this fine facies is formed in the inner ramp. Romero et al. (2002); Corado and Marco (2003) also acknowledge that the presence of red algae and opaque foraminifera indicates a lagoon environment.

**MF4: Bioclastic perforate and imperforate foraminifera packstone-grainstone**

Porous and non-porous foraminifera (Overall 40 – 50%) are the main allochems of this microfacies, among which we can mention *Archaias* sp., *Lepidocyclina* sp., *Rotalia vinoti, Operculina complanata, Borelis* sp., *Pyrgo* sp., *Alveolina* sp. The subordinates of this microstructure are coralline algae (10%), bivalves (5 – 10%), and echinoid spines (5%).

Interpretation: The presence of perforate and imperforate benthic foraminifera, together, indicates a lagoon environment with free water circulation and the absence of a continuous shoal. The grain-supported, abundance of sparite and the diversity of species all confirm this statement. The presence of porcelaneous species such as *Pyrgo* and *Archaias* along with hyaline species, indicates a lagoon with free water rotation in the area of light penetration (euphotic zone) (Nebelsick et al., 2001; Brandano et al., 2010; Morsilli et al., 2012).

**MF5: Bioclast ooid packstone-grainstone**

Bioclasts (20 – 30%) and ooids (25 – 35%) are the major grains of this microfacies, and the major bioclasts identified are benthic foraminifera (such as *Operculina complanata, Archaias* sp., *Lepidocyclina* sp., *Borelis* sp., miliolids), algae (5 – 10%), echinoids (5%), bryozoans (5%), and corals (5%). In addition, peloids and intraclasts are seen in this microfacies.

Interpretation: The identified allochems (like ooid, bryozoans, and corals) and the predominance of sparite in this microfacies indicate an environment with medium to high energy. The presence of ooids, and intraclasts, as well as good sorting and rounding of the grains confirm this. Wilson (1975) and Flügel (2010) consider that the presence of ooids and the absence of muddy ground indicate the formation in an energetic environment such as sand shoal above the normal wave line. The above evidence indicates the formation of this microfacies in the energetic environment of the shoal in the studied sections.

**MF6: Coralline red algae–coral rudstone-floatstone**

The predominant allochems in this microfacies are corallinaceae algae (30 – 40%) and corals larger than 2 mm (20 – 25%); benthic foraminifera (10 – 15%) such as *Borelis inflata, Nephrolepidina praemarginata, Spiroclypeus blanckenhorni, Rotalia* sp., *Amphistegina* sp., *Lepidocyclina* sp. and bryozoans are also found. The space between the grains is filled by micrite and sometimes sparite (in small amounts). Corallinaceae algae are found in the form of rhodolite, crusts, and nodules.

Interpretation: The presence of corallinaceae algae, corals, and large hyaline foraminifera, the large size of these grains, the crushing of some grains, and also the coverage of some corals by algae are important features of this microfacies. At some points in the studied sections, the corals are covered by corallinaceae algae, which indicate meso-oligophotic conditions (Naseri-Karimvand et al., 2019) and stability phase (Kershaw and Brunton, 1999). The small crushing as well as the large size of the grains indicates that these grains did not move much. The crushing is caused by periodic storms on the open sea. The above evidence indicates the formation of this microfacies in the middle ramp.

**MF7: Large benthic foraminifera bioclastic wackestone-packstone**

Large hyaline foraminifera are the main allochems of this microfacies. Species such as *Eulepidina dilatata, Eulepidin* sp., *Lepidocyclina* sp., *Operculina complanata, Operculina* sp., *Rotalia* sp. (Overall 40 – 50%) have been identified in this microfacies. In addition, corallinaceae algae (10%), echinoids (5%), and bryozoans (5%) are also found in this microfacies.

Interpretation: The presence of hyaline species of *Lepidocyclina, Miogypsina*, and *Nummulites*, the large size of these species, and their association with corallinaceae algae indicate a low to medium energy environment with normal salinity. In addition, the stretched appearance of these species indicates the deposition at the beginning of the middle ramp. The diversity and abundance of lens-shaped hyaline species and their association with red algae indicate sedimentation in a light zone environment in the early part of the middle ramp.

(Corado and Marco, 2003; Rasser et al., 2005; Bassi et al., 2007; Barattolo et al., 2007; Shabafrooz et al., 2015; Kakemem et al., 2016; Abyat et al., 2019; Joudaki et al., 2020).

**MF8: Bioclastic Lepidocyclinid-Nummulitid wackestone-packstone**

*Nummulites* and *Lepidocyclina* (Overall 30 – 40%) are the main grains of this microfacies. The predominant species in this microfacies are *Nummulites vascus* and *Lepidocyclina* sp. In addition, hyaline species such as *Operculina complanata, Nephrolepidina* sp., *Nephrolepidina tournoueri, Heterostegina assilinoides, Eulepidina* sp. have also been observed. corallinaceae algae (5 – 10%), bryozoans (5%), and echinoids (5%) are also identifiable in this microfacies. A light amount of planktonic foraminifera of *Globigerina* are also seen.

Interpretation: Many researchers, such as Buxton and Pedly (1989); Geel (2000) attribute the existence of *Nummulites* and *Lepidocyclina* to the open sea and low energy environments (below the FWWB level). *Nummulites* live in an oligotrophic or slightly mesotrophic environment in the open sea at depths of 30 to 80 meters (Langer and Hottinger, 2000; Beavington-Penney and Racey, 2004; BouDagher-Fadel, 2008; Payros et al., 2010). The concomitant presence of *Nummulites* and *Lepidocyclina* along with *Globigerina* indicates the open sea environment. In addition to the above reasons, the diversity of hyaline species (*Nummulites, Lepidocyclina, Nephrolepidina*), the presence of planktonic species, the absence of porcelaneous species, the mud-supported texture, indicate that the MF8 microfacies is formed at the end of the middle ramp.

**MF9: Planktonic foraminifera wackestone–packstone**

Planktonic foraminiferae *Globorotalia* sp. and *Globigerina* sp. (10 – 20%), are the main grains of this microfacies. In addition, echinoids (5 – 10%), bivalvia fragments (5%), and a slight number of benthic foraminifera (5%) are also found in this microfacies. This microfacies is mud-supported and the size of the grains is at the lutite level.

Interpretation: The abundance of the matrix and the presence of planktonic foraminifera indicate a deep, low-energy environment (Buxton and Pedly, 1989; Reading, 1996; Hallock, 1999; Corado and Marco, 2003; Cosovic et al., 2004). In addition, the abundance of planktonic foraminifera indicates eutrophic conditions (Luciani and Cobianchi, 1999). The above reasons and evidence such as the presence of planktonic species, the small number of benthic species, the absence of porcelaneous species, the small size of allochems, the abundance of micrites, and the mud support of this microfacies all indicate that in the studied sections, this microfacies is formed in the outer ramp, and this environment has a low level of energy.

### 5.2 Sedimentary environment

Considering the identified microfacies, the gradual conversion of microfacies to each other, lack of expansion of the shoaling peloidal and ooidal microfacies and the absence of clastic microfacies, the sedimentary environment of the studied sections can be attributed to the carbonate ramp (Fig. 6).

The inner ramp microfacies are MF1: Bioclastic Miliolidae wackestone-packstone, MF2: Imperforate foraminifera wackestone-packstone, MF3-Bioclastic imperforate foraminifera corallinaceae packstone- grainstone, MF4-Bioclastic perforate and packstone-grainstone, MF5-Bioclast ooid packstone-grainstone. The MF1 to MF4 microfacies belong to Lagoon and the MF5 microfacies belong to Shoal.

The main allochems of the inner ramp (lagoon) include large amounts of perforate benthic foraminifera, corallinaceae algae, ostracods, gastropods, and peloids. The abundant presence of porcelain benthic foraminifera such as Miliolidae, *Triloculina trigonula, Quinqueloculina* sp., *Pyrgo* sp., *Austrotrillina asmariensis*, abundant amounts of micrites and support mud of MF1 and MF2 microfacies, indicates the formation of these microfacies in a shallow and low-energy environment with limited water circulation and hypersalinity. Studies such as Wilson (1975); **Hallock1986<empty citation>**; Geel (2000); Romero et al. (2002); Flügel (2010) are also in line with this result. Accordingly, the environment for the formation of these microfacies is an enclosed lagoon. Bioclastic Miliolidae wackestone-packstone (MF1) has been reported by Amirshahkarami (2013) in Ragsefid, Amirshahkarami et al. (2007) in Chaman Bolbol and Kamalifar et al. (2020) in Firoozabad and Bastak. Imperforate foraminifera wackestone-packstone (MF2) has been identified by Avarjani et al. (2015); Kakemem et al. (2016); Abyat et al. (2019); Kamalifar et al. (2020); Joudaki et al. (2020); from the Oligo-Miocene sediments in Zagros.

In the MF3 and MF4 microfacies, the simultaneous presence of perforate (*Lepidocyclina* sp., *Operculina complanata*) and imperforate benthic (*Archaias hensoni, Archaias* sp., *Borelis pygmaea, Quinqueloculina* sp., *Pyrgo* sp.) depositors indicates a lagoon with free water circulation and the absence of a continuous shoal. Nebelsick et al. (2001); Brandano et al. (2010); Morsilli et al. (2012) are also in line with this result. The presence of red algae, the abundance of sparite, the grainstone-packstone background of some microfacies, and the great diversity of species of microfossils also confirm this result. Bioclastic imperforate foraminifera corallinaceae packstone- grainstone (MF3) has been reported by Joudaki et al. (2020) in the Oligo-Miocene sediments in Zagros. He points out that this microfacies have been expanded during the Rupelian to Burdigalian in the Dezful Embayment and during Chattian in the folded and high Zagros. Bioclastic perforate and imperforate foraminifera packstone-grainstone (MF4) has been identified by Kakemem et al. (2016); Abyat et al. (2019); Kamalifar et al. (2020); Joudaki et al. (2020) from the Oligo-Miocene sediments in the Zagros.

In shoal, bioclasts and ooids are the main grains, along with peloids and intraclasts, corallinaceae algae, echinoids, bryozoans, and corals (MF5). These allochems, abundant sparite, high sorting, and roundness of the grains, confirm the high energy level of this environment. Bioclast ooid packstone-grainstone (MF5) has been identified by Vaziri-Moghaddam et al. (2010); Sahraeyan et al. (2014); Joudaki et al. (2020) in Asmari Formation.

MF6-Coralline red algae–coral rudstone-floatstone,

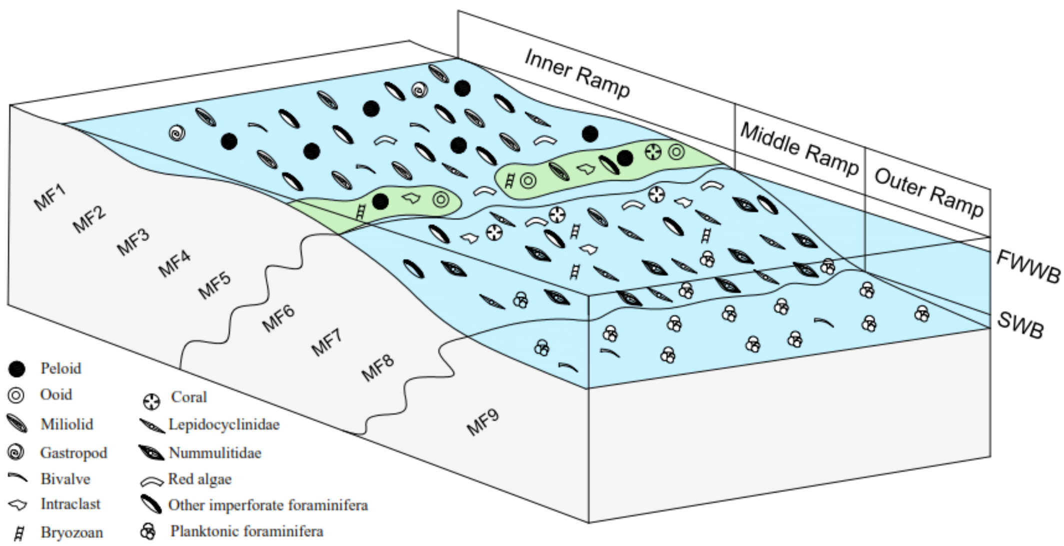


**Figure 6.** Distribution of microfacies in the sedimentary environment of Middle Eocene to Early Miocene deposits in the studied sections.

MF7- Large benthic foraminifera bioclastic wackestone-packstone, MF8- Bioclastic Lepidocyclinid-Nummulitid wackestone-packstone microfacies belong to the middle ramp. Large hyaline foraminifera (*Nummulites vascus, Eulepidina dilatata, Eulepidina* sp., *Nephrolepidina* sp., *Nephrolepidina tournoueri, Operculina complanata, Rotalia* sp.), corallinaceae algae and corals are the main grains of this environment.
The existence of large hyaline species (*Lepidocyclina, Miogypsina*, and *Nummulitidae*), elongated shape of these species, large size of allochems, their association with corallinaceae algae, species diversity and abundance, presence of few planktonic species and absence of porcelaneus species indicate the low to medium energy environment in the middle ramp. Many researchers, such as Shabafrooz et al. (2015); Kakemem et al. (2016); Abyat et al. (2019); Joudaki et al. (2020) have reported microfacies with such features as belonging to the Oligo-Miocene middle ramp in Zagros. The presence of large, broad, elongated hyaline foraminiferae with red algae indicates their formation in the middle ramp (**Vennin2003**). Coralline red algae–coral rudstone-floatstone (MF6) has been reported in Oligo-Miocene sediments in Zagros Basin by Vaziri-Moghaddam et al. (2010); Sahraeyan et al. (2014); Avarjani et al. (2015); Naseri-Karimvand et al. (2019); Abyat et al. (2019). Large benthic foraminifera bioclastic wackestone-packstone (MF7) has been identified in Oligo-Miocene sediments in Zagros Basin by Vaziri-Moghaddam et al. (2006); Amirshahkarami et al. (2007); Abyat et al. (2019); Kamalifar et al. (2020); Joudaki et al. (2020). Bioclastic Lepidocyclinid-Nummulitid wackestone-packstone (MF8) This microfacies has been reported in the Oligo-Miocene sediments in Zagros by Kakemem et al. (2016); Kamalifar et al. (2020); Joudaki et al. (2020).
Microfacies MF9- planktonic foraminifera wackestone–packstone belongs to the outer ramp. The main allochemes of this microfacial are planktonic foraminifera Such as *Globorotalia* sp., *Globigerina* sp. The presence of planktonic species, the small number of benthic species, the abundance of the matrix, and the supportive mud indicate a deep, low-energy environment such as the outer ramp. Such features have also been assigned to the outer ramp by Buxton and Pedly (1989); Reading (1996); Hallock (1999); Corado and Marco (2003); Cosovic et al. (2004). A microfacies similar to this one has been reported in Oligo-Miocene sediments in Zagros Basin by Vaziri-Moghaddam et al. (2006); Amirshahkarami et al. (2007); **Sadeghi2011<empty citation>**; Abyat et al. (2019); Kamalifar et al. (2020); Joudaki et al. (2020).

## 6. Discussion

In the Isa Abad section lagoon, shoal, middle ramp, and outer ramp environments have been recognized. In the meantime, the microfacies of the middle ramp environment have an abundance maximum of %43. In the following, order: the lagoon's microfacies with %28 shoal 's microfacies with %16, and outer ramp's microfacies with %13 are the next categories. In this section, MF7 (Large benthic foraminiferal bioclastic wackestone-packstone) belongs to the middle ramp with an abundance %33 and then MF5 (Bioclast ooid packstone-grainstone) belongs to the shoal with %17 has the highest abundance among facies.
In the Gahroo section, the lagoon, shoal (very limited), and the middle ramp environments are expanding. Lagoon's microfacies with %51 and then the middle ramp's microfacies with %48 have the highest abundance in this section. Shoal's microfacies have the lowest abundance percentage with %1. MF7 (Large benthic foraminiferal bioclastic wackestone-packstone) belonging to the middle ramp with %48 and then the MF3 (Bioclastic imperforate foraminifera corallinacea packstone-grainstone) belonging to the lagoon with %24 have the highest frequency among the facies of Gahroo section (Fig. 7).
In Isa Abad sections, sediments of Jahrom Formation are from middle to upper Eocene age (Zulnoorian et al., 2023), and were deposited in middle ramp and upper ramp environments. The sediments of the Asmari Formation in this section are Rupelian to Burdigalian (Zulnoorian et al., 2023), and are formed in the middle and outer ramp. In a vertical comparison, in this section, the Jahrom Formation is formed in a deeper environment than the Asmari Formation. In the Gahroo section, the sediments of the Jahrom Formation were deposited in the middle to upper Eocene (Zulnoorian et al., 2023) in the inner ramp and middle ramp environments. The sediments of the outer ramp that were identified in the Jahrom Formation in the Isa Abad section were not observed in this section. Rupelian to Burdigalian sediments of the Asmari Formation (Zulnoorian et al., 2023) in the Gahroo section were formed in the inner ramp. Of course, Middle ramp sediments were also identified with a much less expansion at the base of the Asmari Formation. The difference between Rupelian and Burdigalian sediments in these two sections is the abundance of inner ramp microfacies in Isa Abad compared to the Gahroo section. In both sections, a retrograde trend can be seen, that, finally, leads to the disconformity contact between Asmari and Gachsaran formations.
In Fig. 8, the sedimentary environment of these Jahrom and Asmari formations was compared. In a comparison between both sections, there is more facies variety in the Isa Abad section than in the Gahroo section. So, 9 microfacies in the Isa Abad section and 6 microfacies in the Gahroo section were recognized. In the Isa Abad section, wackestone, packstone, grainstone, and also, boundstone microfacies can be identified. But, in the Gahroo section, only wackestone, packstone, and grainstone microfacies can be seen. In addition due to the lake of outer ramp microfacies and also the abundance of lagoon microfacies in the Gahroo section, as a result, this section is formed in a shallower environment than the Isa Abad section.
For comparison, sediments of Jahrom and Asmari formations in the studied sections with the other High Zagros sections, Tuf-e sefid section in the north of chelgerd, Agha seyed, in the Farsan, Shoorom, Semirom, Pir ghar, Hamzeh Ali in the west of borojen and Shalamzar, Saldoran and Dasht-e Zari (west of Shahr-e kord) were selected (Table 3). Babazadeh and Jamsahk (2018) believe that the Eocene-aged Jahrom Formation was formed in the Pir ghar section

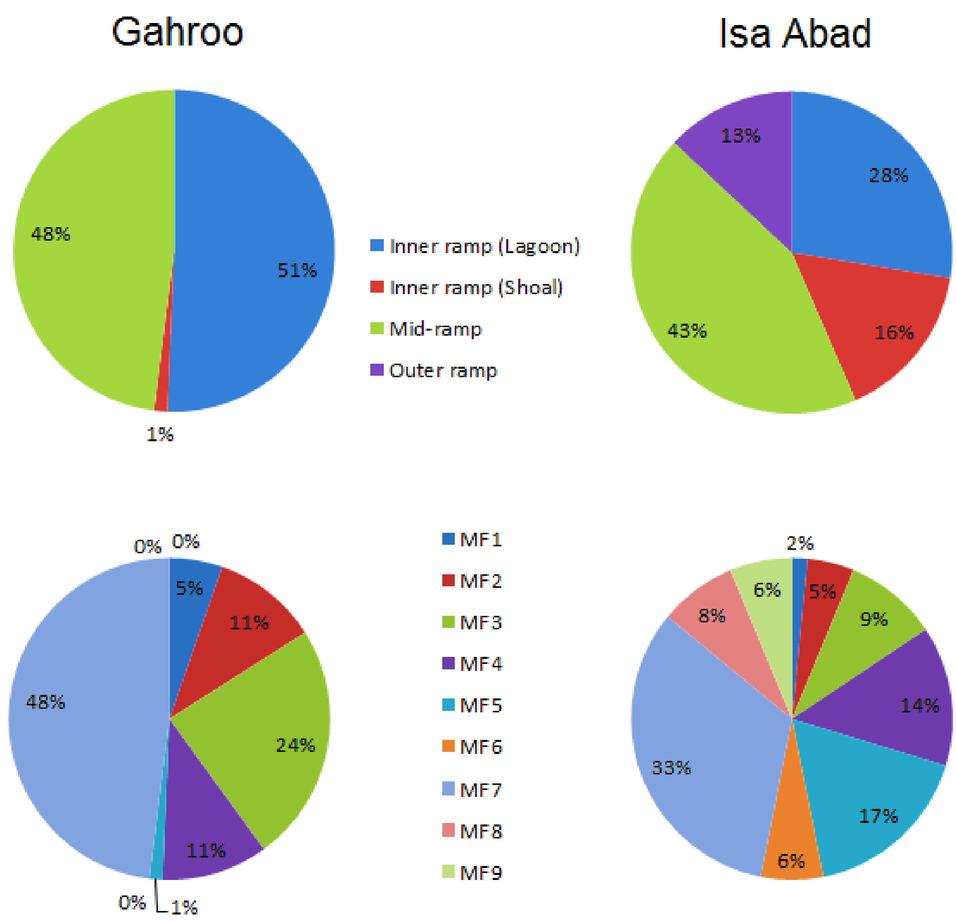


**Figure 7.** The abundance of microfacies and sedimentary environments has been identified in the studied sections.

in the Southwest of Shahr-e Kord in the inner ramp (Lagoon and shoal), open sea and deep basin environments. Sediments of the Jahrom Formation (Early-middle Eocene) of the Hamzeh -Ali and Shalamzar sections were formed in the inner ramp (Lagoon and coastal plain), middle ramp, and outer ramp environments (Almasinia, 2018). Soltani Najafabadi et al. (2018) have been interpreting the sedimentary environment of the Jahrom Formation (Early-middle Eocene) in the Saldoran, Dasht-e Zari sections as inner ramp (Tidal flat, lagoon, shoal), middle ramp, outer ramp, and basin. In the Tuf-e Sefid section, sediments of the Asmari Formation (Rupelian) were formed in the outer ramp environments (Seyrafian et al., 2011). Rupelian- Chattian sediments have been studied by Hamidzadeh et al. (2017) in the Agha seyed section that denotes the existence of three belts of the inner ramp (Littoral and back shoal), middle ramp (Shoal, patch reef), and outer ramp (Distal and proximal). Khanali and Seyrafian (2012) state Chattian to Burdigalian sediments of Shoorom section were formed in the inner and middle ramp environments. Chattian sediments of the Semirom section were formed in the inner ramp (Lagoon) environment (Joudaki et al., 2020).

Kabir kuh-Dareh Shahr, Sepid Dasht, Mamoolan, and Dehloran sections in the Lorestan basin were studied by Vaziri-Moghaddam et al. (2010). Rupelian sediments are not observed in all sections and Chattian to Aquitanian sediments are not observed in the Mamoolan and Sepid Dasht sections, this indicates the absence of sedimentation. In the Kabir kuh-Dareh Shahr section, were identified middle and outer ramp environments in Chattian and also, inner and outer ramp environments in Aquitanian. In the Sepid Dasht section, sediments had deposited in the middle and outer ramp environment in Burdigalian. In the Dehloran section, Vaziri-Moghaddam et al. (2010) have suggested an inner ramp (Tidal flat and lagoon), middle ramp and outer ramp in early Aquitanian, and inner ramp (often the lagoon) in late Aquitanian to Burdigalian. In the Mamoolan section, have been suggested middle and outer ramp environment in Burdigalian. Rajabi et al. (2021) identified the inner, middle, and outer ramp environment for the Asmari Formation in the Makhmal Kuh section from Rupelian to Aquitanian stages.

In the Izeh zone, the Bangestan, Tang-e Ban, Tang-e Sapou (Roozpeykar and Moghaddam, 2015), Genaveh, northeast of Dehdasht, Arand, Siang (Naseri-Karimvand et al., 2019) and Rig anticline (Kakemem et al., 2016) sections were selected for comparison. Asmari Formation sediments in Bangestan (Aquitanian-Burdigalian) had deposited in the inner ramp (Lagoon and shoal) environment, in Tang-e Ban (Chattian-Burdigalian) had deposited in the inner ramp (Lagoon) and in Tang-e Sapou (Chattian-Burdigalian) had deposited in the inner ramp (Lagoon). In the Genaveh, north-

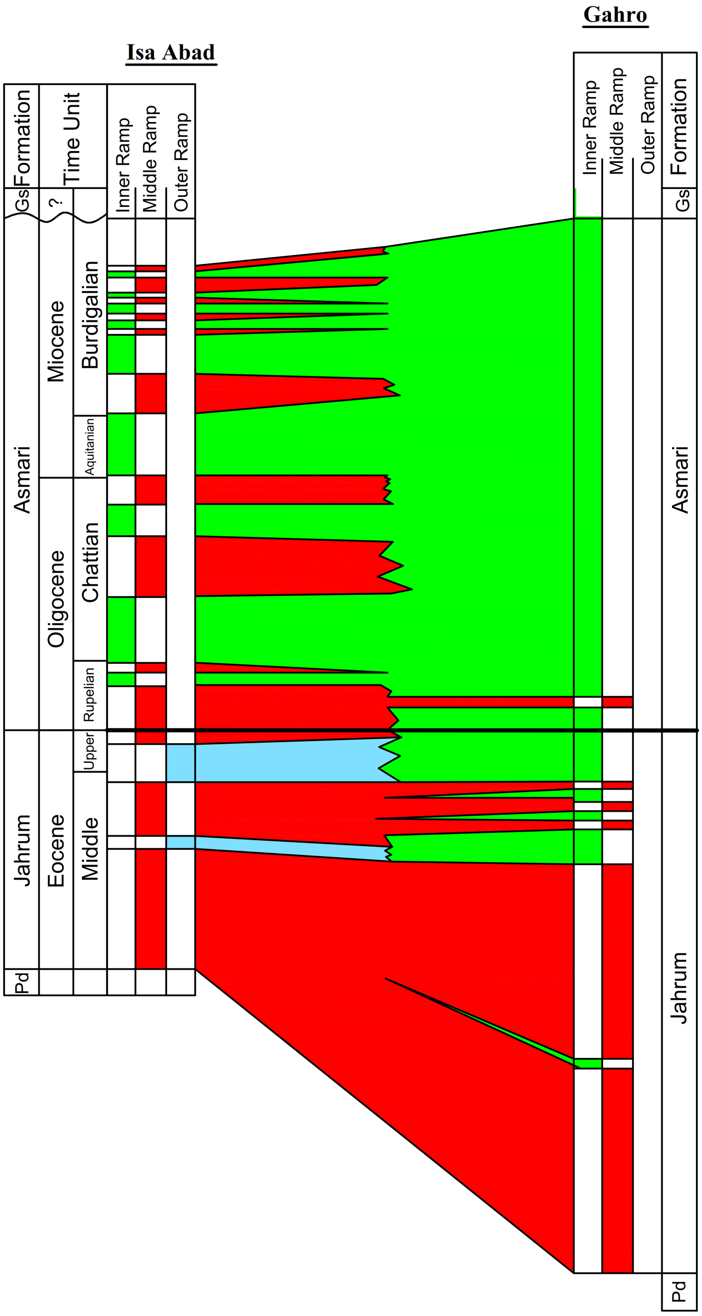


**Figure 8.** Correlation of sedimentary environments of Jahrom and Asmari formations in the studied sections.

east of Dehdasht, Arand, and Siang sections, Oligocene sediments have deposited in the inner, middle, and outer ramp, Aquitanian sediments have deposited in the inner and middle ramp and Burdigalian sediments have deposited in the inner ramp environments. In the Rig anticline, Asmari Formation sediments have formed in the inner ramp (Tidal flat and lagoon), middle ramp (Shoal), outer ramp, and basin.

Nargesi, Kilorkarim, Marun, and Zeloi oil fields in Dezful Embayment were chosen sections for comparison. Sediments of the Jahrom Formation in the Nargesi oil field (south of the Dezful Embayment) were formed in the inner ramp (Supratidal, intertidal, Lagoon, and Shoal), middle ramp, and outer ramp (Ahmadi et al., 2022). Sediments of Asmari Formation (Chattian to Burdigalian) in Marun oil field have deposited in inner ramp (Supratidal, intertidal, lagoon and shoal), middle and outer ramp (Avarjani et al., 2015) and in Zeloi oil field (Aquitanian to Burdigalian) have formed in inner ramp (Tidal flat, shoal and lagoon), middle and outer ramp (Abyat et al., 2019). In the Kilorkarim oil field sediments of this formation indicate sedimentation in the inner ramp (Tidal flat and lagoon), middle ramp (Bar/shoal), and outer ramp (Mirzaee Mahmoodabadi, 2023), and in the Nargesi oil field are indicative the inner ramp environment (Supratidal, intertidal, lagoon and shoal). Khatibi mehr et al. (2012) in Fars, suggest the sedimentary environment of Jahrom Formation (Early Paleocene -late Eocene) in the southeastern Lar (Kuh-e Gach section) as

**Table 3.** Comparison of the sedimentary environments of Jahrom and Asmari formations identified in the studied sections with other sections of High Zagros.

| Section | Author | Formation | Age | Inner ramp | Middle ramp | Outer ramp |
|---|---|---|---|---|---|---|
| **Pirghar** | Babazadeh and Jamsahk (2018) | Jahrom | U.Eoc | | | |
| **Hamzeh Ali** | Almasinia (2018) | | L.M.Eoc | | | |
| **Shalamzar** | Almasinia (2018) | | M.Eoc | | | |
| **Dasht-Zari** | Soltani Najafabadi et al. (2018) | | L.M.Eoc | | | |
| **Saldoran** | Soltani Najafabadi et al. (2018) | | L.M.Eoc | | | |
| **Isa Abad** | this study | | M.U.Eoc | | | |
| **Gahroo** | this study | | M.U.Eoc | | | |
| | | | | | | |
| **Tuf-e Sefid** | Seyrafian et al. (2011) | Asmari | Rup. | | | |
| **Agha Seyed** | Hamidzadeh et al. (2017) | | Rup.-Chat. | | | |
| **Shurum** | Khanali and Seyrafian (2012) | | Chat.-Burd. | | | |
| **Semirom** | Joudaki et al. (2020) | | Rup.-Burd. | | | |
| **Isa Abad** | this study | | Rup.-Burd. | | | |
| **Gahroo** | this study | | Rup.-Burd. | | | |

inner ramp (Tidal flat, lagoon, and shoal) and middle ramp. In the Tang-e Nimbashi section, west of Estahban sediments of the Jahrom Formation (Late Paleocene?-middle Eocene) are formed in the inner ramp (Supratidal, intertidal, and lagoon), middle and outer ramp (Sadeghi and Jokar, 2018). Sediments of Jahrom Formation (Middle-late Eocene), in the Cheleh gah Sepidan section (Northwest Shiraz), have deposited in the inner ramp (lagoon and shoal), middle ramp, and open sea environments (Parvaneh Nejad Shirazi et al., 2020). Moallemi et al. (2010) investigated sediments of the Jahrom Formation (Late Eocene) in the Kuh-e Gisakan in Borazjan and nearby the oil fields. The sedimentary environment of this formation was introduced as the inner, middle, and outer ramp. In these sections has been identified Hemiplagic to Pelagic facies related to the gradual passage of Pabdeh and Jahrom formations. Yazdanpanah et al. (2022) in Gousheh-Nekan, Chehel Cheshmeh, and Tang-e Garm sections (Interior Fars), have introduced the sedimentary environment of Jahrom Formation, (Early–middle Eocene) inner ramp (Tidal zone, lagoon and shoal). Kamalifar et al. (2020) in the Firoz Abad and Bastak sections suggested inner ramp (Tidal flat and lagoon), middle ramp (Shoal), and outer ramp environment for the Asmari Formation (Rupelian to Aquitanian). Kalanat et al. (2014) also state that the Asmari Formation (Rupelian to Chattian) formed in the inner ramp (Lagoon and shoal), middle and outer ramp environments, in the Firoz Abad section.

Supratidal and intertidal microfacies containing anhydrite, stromatolite boundstone, fenestral mudstone, dolomudstone, quartz arenite are reported in many sections of Zagros Basin such as **Maghfouri2022<empty citation>** in Lorestan, Mirzaee Mahmoodabadi (2023) in Kilorkarim field, Ahmadi et al. (2022) in the southern part of Dezful Embayment, **Joudaki2021<empty citation>** In Persian Gulf Forland, Kamalifar et al. (2020) in Fars, Abyat et al. (2019) in Zeloi oilfield, Kakemem et al. (2016) in Izeh Zone, **Avarjani2014<empty citation>** in North of Dezful Embayment, Kalanat et al. (2014) in Fars, Vaziri-Moghaddam et al. (2010) in Lorestan, but, similar to the upper microfacies were not observed in Gahroo and Isa Abad sections. The absence of Ahvaz sandstone Member is the difference between these sections and the sections in the south of the Dezful embayment. Also absence of evaporate sediments of Kalhor Member is the difference between these sections and the southwest sections of the Lorestan basin and the northern part of Dezful Embayment.

In the northern belt of the Tethys, extensive LBF-rich carbonate ramps dominate these environments, where broad LBF-rich platforms developed from the Pyrenean realm to the Tibetan sector, across the Alps, Adriatic Platform, Apennines, Carpathians, Caucasus, Helenian, Anatolian and Indian domains, at paleolatitudes between 35° and 45°N (**MartinMartin2001**; Hontzsch et al., 2013; Martin-Martin et al., 2020, 2021; Tosquella et al., 2022). LBF carbonate platforms developed on the southern Tethyan margin between Morocco and the Oman-Yemen domains at paleolatitudes ranging from 20°N and the equator (Hontzsch et al., 2013; Martin-Martin et al., 2020, 2021; Tosquella

et al., 2022).
Wide shallow-marine carbonate platforms developed during the Eocene in the circum-Tethyan sectors. In these broad carbonate shallow-marine areas, larger benthic foraminifera (LBF) rim facies developed, which were dominated by nummulites and coralline algae. Contrarily, coral patch reefs usually decreased or disappeared during these warming events (Martin-Martin et al., 2020, 2021).
Tosquella et al. (2022) and Martin-Martin et al. (2021) identified inner, middle, and outer ramp environments in Western Tethyan. The differences between the sections of Isa Abad and Gahroo with the aforementioned researches of the western Tethyan are: it can be pointed to the absence of quartz arenite, framestone, and boundstone microfacies in these sections. The similarities of the studies about the aforementioned sections with western Tethyan are Existing microfacies containing LBF, red algae, and coral. Open sea microfacies containing planktonic foraminifera that were reported in the sections of western Tethyan which were identified in the Isa Abad section but in the Gahroo section were not identified (MF9).
In Isa bad and Gahroo sections photozoan facies have a lot of expansion and heterozoan facies have been identified in them. Coletti et al. (2022) pointed to the expansion of photozoan facies in the Eocene to the Miocene in the south of Tethyan. Their studies consider most of the facies found in the sediments of Paleocene to Miocene to be respectively: Larger Benthic Foraminifera (LBF), Red Calcareous Algae (RCA), and Colonial Corals (CC). The maximum frequency of LBF facies exists in the shallow carbonate platforms in the Eocene and then in the Oligocene and Miocene.
In the Isa Abad and Gahroo sections, LBF facies can be seen as abundant in the Eocene to Miocene. RCA facies are more abundant in the Oligocene and then in the Miocene. The amount of these facies has decreased in the Eocene. RCA facies are not seen in the sediments of the Jahrom Formation of the Eocene in the studied sections in this research while these facies were identified in the Asmari Formation (Oligocene to early Miocene). This distribution is consistent with the results of Coletti et al. (2022) studies. The abundance model of RCA facies is similar to CC facies. So, the RCA facies, also, has a minimum abundance in the Eocene and a maximum abundance in the Oligocene (Coletti et al., 2022) (Table 4). Calcareous Algae Green (GCA) facies identified in other places of Tethyan were not observed in these sections.

## 7. Conclusion

Middle Eocene to Early Miocene sediments (Jahrom and Asmari formations) have been formed in the Isa Abad section with actual thickness of 151.5 m including limestones and with fossil-containing and nodular sand limestones and in the section of Imamzadeh Gahroo section with the actual thickness of 179 m of limestone and fossil-containing mass. In these sections, a total of 9 sedimentary micro-facies were identified in three micro-facies belts of inner ramp, middle ramp and outer ramp. Evidence such as the gradual conversion of microfacies to each other, the lack of abundant expansion of the shoaling ooid and peloid microfacies, and the absence of turbidite and slumping structures suggest the sedimentary environment of the homoclinal ramp for these deposits. The allochems in lagoons are the imperforate benthic media, corallinaceae algae, ostracoda, gastropods, and peloids, those in shoal are bioclasts, ooids, peloids, intraclasts, corallinaceae algae, echinoids, bryozoans, and corals, in the middle ramp they are large hyaline species and corallinaceae algae, and in the outer ramp they are planktonic species and dominant allochems. In Isabad section, the inner and middle ramp microfacies have the highest frequency, and the outer ramp microfacies have the lowest frequency. In Gahroo section, the inner ramp and middle ramp microfacies have the highest frequency. The outer ramp microfacies are not seen in this section. The results show that the Middle Eocene to Early Miocene sedimentary environment is deeper in Isa Abad than the Gahroo section.

**Table 4.** Percent distribution of the main groups of carbonate grains (dominated plus co-dominated facies) during the Palaeocene, Eocene, Oligocene, Miocene, following the section- average and the formation- average approaches, respectively (Coletti et al., 2022).

| Dominated + codominated facies | LBF | CC | RCA | GCA | EBF | Ooids and Peloids | Mud | Microbial crust | Heterozoan |
|---|---|---|---|---|---|---|---|---|---|
| Section-average% | | | | | | | | | |
| Palaeocene | 63.9 | 6.07 | 25.69 | 18.5 | 0 | 3.31 | 1.33 | 0.24 | 14.43 |
| Eocene | 81.7 | 0.61 | 4.07 | 2.39 | 0.34 | 2.95 | 3.88 | 0.13 | 10.43 |
| Oligocene | 70.24 | 14.71 | 28.49 | 0 | 1.8 | 7.81 | 0 | 0 | 7.91 |
| Miocene | 42.2 | 4.65 | 12.33 | 0 | 0.05 | 7.58 | 15.72 | 0.13 | 29 |
| Section-average% | | | | | | | | | |
| Palaeocene | 60 | 2.36 | 26.03 | 17.82 | 0 | 2.54 | 2.31 | 0.26 | 13.95 |
| Eocene | 81.61 | 0.51 | 5.54 | 1.83 | 2.54 | 3.11 | 2.04 | 0.13 | 10.21 |
| Oligocene | 85.95 | 36.61 | 16.37 | 0 | 0.34 | 3.19 | 0 | 0 | 5.05 |
| Miocene | 29.27 | 21.42 | 21.22 | 0 | 0 | 8.59 | 5.36 | 0.02 | 37.63 |

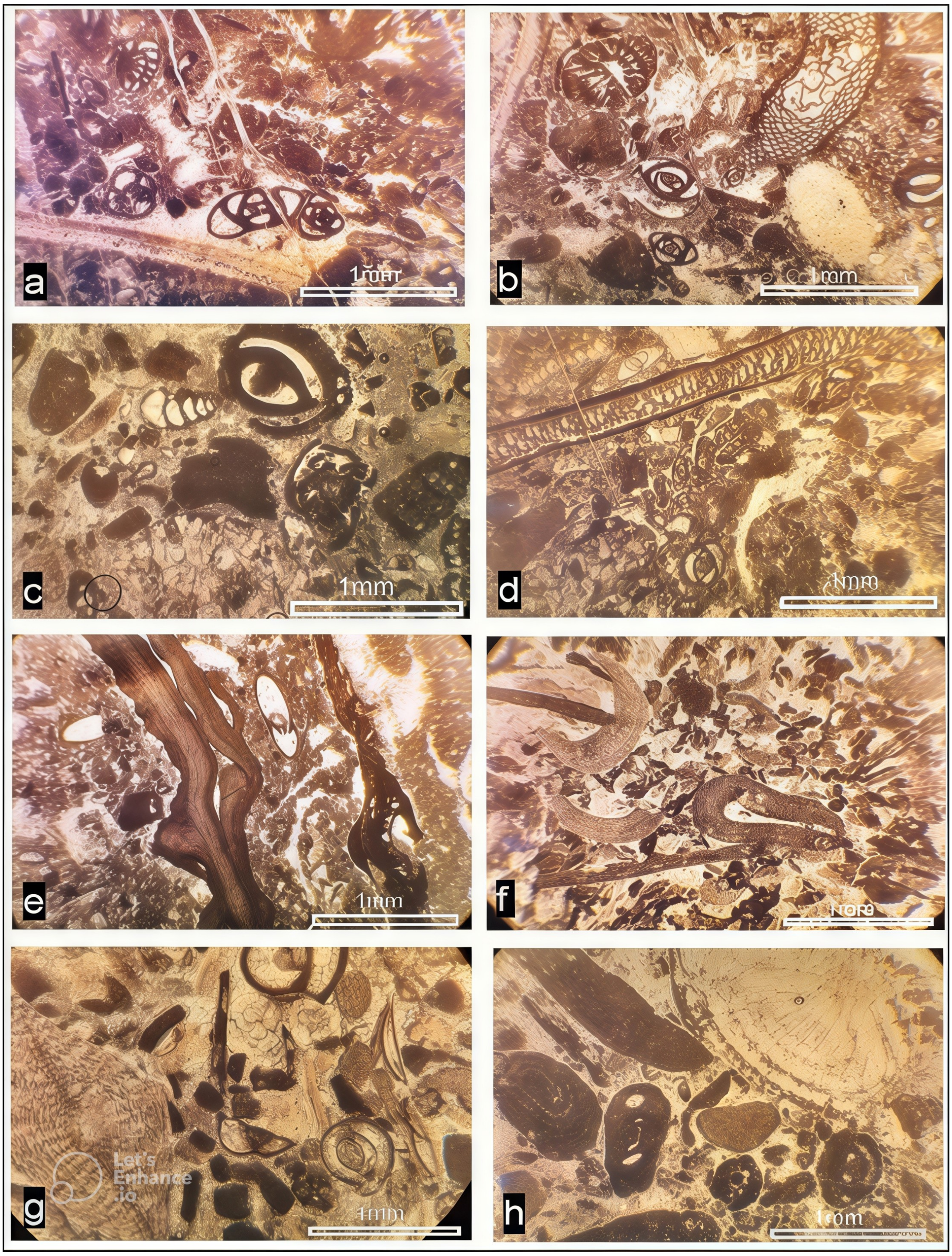


**Plate 1.** (a) Microfacies MF1: Bioclastic Miliolidae wackestone-packstone in Isa Abad section (b) Microfacies MF1: Bioclastic Miliolidae wackestone-packstone in Gahroo section (c) Microfacies MF2: Imperforate foraminifera wackestone-packstone in Isa Abad section (d) Microfacies MF2: Imperforate foraminifera wackestone-packstone in Gahroo section (e) Microfacies MF3-Bioclastic imperforate foraminifera corallinacea packstone- grainstone in Isa Abad section (f) Microfacies MF3-Bioclastic imperforate foraminifera corallinacea packstone- grainstone in Gahroo section (g) Microfacies MF4-Bioclastic perforate and imperforate foraminifera packstone-grainstone in Isa Abad section (h) Microfacies MF4- Bioclastic perforate and imperforate foraminifera packstone-grainstone in Gahroo section.

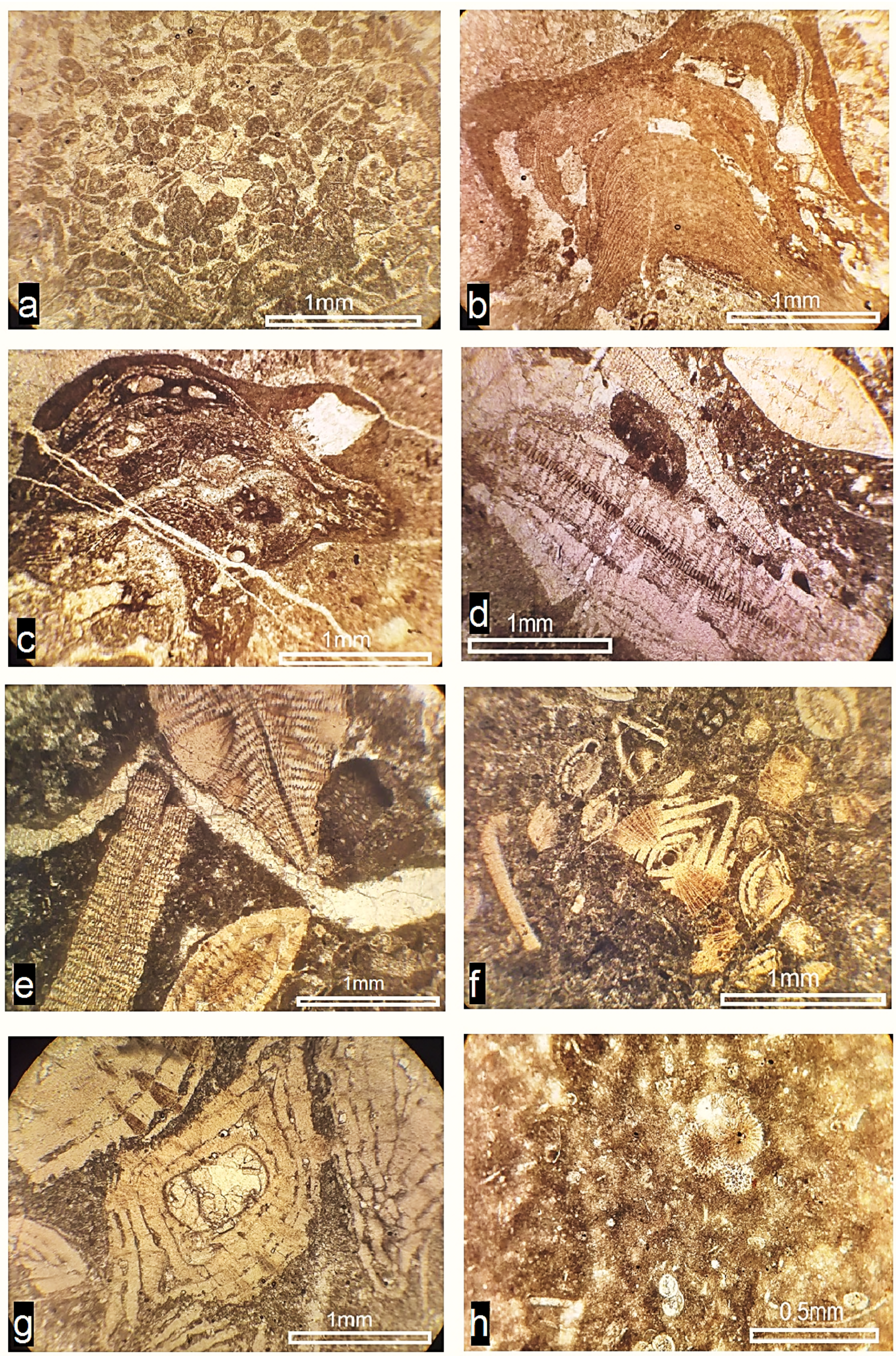


**Plate 2.** (a) Microfacies MF5- Bioclast ooid packstone-grainstone in Gahroo section (b) Microfacies MF6-Coralline red algae–coral rudstone-floatstone in Isa Abad section (c) Microfacies MF6-Coralline red algae–coral rudstone-floatstone in Isa Abad section (d) Microfacies MF7- Large benthic foraminifera bioclastic wackestone-packstone in Isa Abad section (e) Microfacies MF7- Large benthic foraminifera bioclastic wackestone-packstone in Gahroo section (f) Microfacies MF8- Bioclastic Lepidocyclinid-Nummulitid wackestone-packstone in Gahroo.

**Authors contributions**
Authors have contributed equally in preparing and writing the manuscript.

**Availability of data and materials**
The data that support the findings of this study are available from the corresponding author, upon reasonable request.

**Conflict of interests**
The authors declare that they have no known competing financial interests or personal relationships that could have appeared to influence the work reported in this paper.

## References

Abyat Y., Abyat A., Abyat A. (2019) Microfacies and depositional environment of Asmari formation in the Zeloi oil field, Zagros basin, south-west Iran. *Carbonates and Evaporites* 34 (2): 15–28. DOI: https://doi.org/10.1007/s13146-019-00507-1.

Ahmadi Y., Rahimpour-Bonab H., Mehrabi H., Omidpour A. (2022) Comparison of sedimentation-diagenesis history of Paleocene-Miocene succession (Jahrom and Asmari formations) in the southern part of Dezful Embayment. *Applied Sedimentology* 10 (20): 26–53. DOI: https://doi.org/10.22084/psj.2022.25306.1320.

Alavi M. (2004) Regional stratigraphy of the Zagros fold-thrust belt of Iran and its proforeland evolution. *American Journal of Sciences* 304:1–20. DOI: https://doi.org/10.2475/AJS.304.1.1.

——— (1994) Tectonics of the Zagros Orogenic Belt of Iran: New data and interpretation. *Tectonophysics* 229:211–238. DOI: https://doi.org/10.1016/0040-1951(94)90030-2.

Allahkarampour Dill M., Vaziri-Moghaddam H., Seyrafian A., Behdad A. (2018) Oligo-Miocene carbonate platform evolution in the northern margin of the Asmari intra-shelf basin, SW Iran. *Marine and Petroleum Geology* 92:437–461. DOI: https://doi.org/10.1016/j.marpetgeo.2017.11.008.

Almasinia M. (2018) Middle Eocene carbon and oxygen isotopes sequence stratigraphy high Zagros Jahrom formation microfacies. *Researches in Earth Sciences* 5 (2): 38–49.

Amirshahkarami M. (2013) Microfacies correlation analysis of the Oligocene-Miocene Asmari Formation in the central part of the Rag-e-Safid anticlinal oil field, Zagros Basin, south-west Iran. *Turkish Journal of Earth Sciences* 22:204–219.

Amirshahkarami M., Vaziri-Moghaddam H., Taheri A. (2007) Sedimentary facies and sequence stratigraphy of the Asmari Formation at Chaman-Bolbol, Zagros Basin Iran. *Journal of Asian Earth Science* 29 (5-6): 947–959.

Arjmandzadeh R., Teshnizi E. S., Ahmadi A. A., Mahdavi A., Tavsoli S., Dabiri R. (2020) The mineralogy, geochemistry and genesis of Aghol-Messi sedimentary copper - uranium deposit, Tabas block, Central Iran. *Researches in Earth Sciences* 11 (4): 47–70. DOI: https://doi.org/10.52547/esrj.11.4.47.

Avarjani S., Mahboubi A., Moussavi-Harami R., Amiri-Bakhtiar H., Brenner R. L. (2015) Facies, depositional sequences, and biostratigraphy of the Oligo-Miocene Asmari formation in Marun oil field, North Dezful Embayment, Zagros Basin, SW Iran. *Palaeo world* 24:336–358.

Babazadeh S. A., Jamsahk H. (2018) Microfacies analysis of Jahrom formation in the southwest of Shahr-e Kurd city, Pirghar section. *21st Conference of Geological Society of Iran*

Barattolo F., Bassi D., Romero R. (2007) Upper Eocene larger foraminiferal coralline algal facies from the Klokova Mountain (south continental Greece). *Facies* 53:361–375.

Bassi D., Hottinger L., Nebelsick J. H. (2007) Larger foraminifera from the upper Oligocene of the Venetian area, north-east Italy. *Palaeontology* 50:845–868. DOI: https://doi.org/10.1111/j.1475-4983.2007.00677.x.

Beavington-Penney S. J., Racey A. (2004) Ecology of extant nummulitids and other larger benthic foraminifera. Applications in Paleoenvironmental analysis. *Earth-Science Reviews* 67 (3-4): 219–265.

Berberian M., King G. C. P. (1981) Towards a paleogeography and tectonic evolution of Iran. *Canadian Journal of Earth Sciences* 18:210–265. DOI: https://doi.org/10.1139/e81-019.

BouDagher-Fadel M.K. (2008) Evolution and geological significance of larger benthic foraminifera. 21:540. Developments in Palaeontology and Stratigraphy Elsevier

Boukhary M., Abdelghany O., Hussein-Kamel Y., Bahr S., Alsayigh A., Abdelraouf M. (2010) Oligocene larger foraminifera from United Arab Emirates, Oman and Western Desert of Egypt. *Historical Biology* 22:348–366. DOI: https://doi.org/10.1080/08912960903570047.

Brandano M., Frezza V., Tomassetti L., Pedley M. (2010) Facies analysis and paleoenvironmental interpretation of the Late Oligocene Attard Member (Lower Coralline Limstone Formation), Malta. *Sedimentology* 56:1138–1158.

Buxton M. W. N., Pedly H. M. (1989) Short paper, A standardized model for Tethyan Tertiary carbonate ramps. *Journal of Geological Society of London* 146:746–748.

Cahuzac B., Poignant A. (1997) An attempt of biozonation of the European basin, by means of larger neritic foraminifera. *Bulletin de la Société Géologique de France* 168 (2): 155–169.

Coletti G., Commissario L., Mariani L., Bosio G., Desbiolles F., Soldi M., Bialik O. (2022) Palaeocene to Miocene southern Tethyan carbonate factories: A meta-analysis of the successions of South-western and Western Central Asia. *The Depositional Record* 8 (3): 1031–1054. DOI: https://doi.org/10.1002/dep2.204.

Corado L., Marco B. (2003) Aphotic zone carbonate production on a Miocene ramp, Central Apennines, Italy. *Sedimentary Geology* 161:55–70.

Cosovic V., Drobne K., Moro A. (2004) Paleoenvironmental model for Eocene foraminiferal limstones of the Adriatic carbonate platform (Istrian Peninsula). *Facies* 50:61–75.

Doski J. A. H., Mc Clay K. (2022) Tectono-stratigraphic evolution, regional structure and fracture patterns of the Zagros fold-thrust belt in the Duhok region, Kurdistan, northern Iraq. *Tectonophysics* 38:229506. DOI: https://doi.org/10.1016/j.tecto.2022.229506.

Dunham R. J. (1962) Classification of carbonate rocks according to their depositional texture. Edited by Ham W.E., 108–121. AAPG Bulletin

Embry A. F., Klovan J. E. (1971) A late Devonian reef tract on northeastern Banks Island, NWT. *Bulletin of Canadian Petroleum Geology* 19:730–81.

Ferràndez-Caadell C., Bover-Arnal T. (2017) Late Chattian larger foraminifera from the Prebetic Domain (SE Spain): new data on Shallow Benthic Zone 23. *Palaios* 32:83–109. DOI: https://doi.org/10.2110/palo.2016.010.

Flügel E. (2010) Microfacies of carbonate rocks, analysis, interpretation and application. 2nd 976. Springer

Geel T. (2000) Recognition of stratigraphic sequences in carbonate platform and slope deposits: Empirical models based on microfacies analysis of Paleogene deposits in southeastern Spain. *Palaeogeography, Palaeoclimatology, Palaeoecology* 155:211–238.

Habibi T. (2016a) Bio- and sequence stratigraphy and microfacies analysis of the Oligocene Asmari formation at Sepidar Anticline, Interior Fars sub-Basin, SW Iran. *Historical Biology* 28 (4): 519–532. DOI: https://doi.org/10.1080/08912963.2014.990388.

——— (2017) Biostratigraphy and systematic Paleontology of the Oligocene larger benthic foraminifera from Fars Province, Zaros Basin, SW Iran. *Iranian Journal of Science and Technology* 42:1285–1308. DOI: https://doi.org/10.1007/s40995-017-0155-7.

——— (2016b) Biostratigraphy, paleoenvironment and foraminiferal associations of the Rupelian–Chattian sediments in Zagros Basin, SW Iran. *Journal of African Earth Sciences* 323:370–380. DOI: https://doi.org/10.1016/j.jafrearsci.2016.08.007.

Hallock P. (1999) Symbiont-bearing foraminifera. Edited by Sen Gupta B.K. *Modern foraminifera*

Hamidzadeh S. M., Babazadeh A., Asgari-Pirbaluti B., Solgi A. (2017) Microfacies analysis and depositional environments of the Asmari Formation at the Ghar-e Agha Seyyed section, Farsan area (Chaharmahal Bakhtiari province), High Zagros. *Scientific Quarterly Journal of Geosciences* 27 (105): 25–32. DOI: https://doi.org/10.22071/gsj.2017.54127.

Heydari E. (2008) Tectonics versus eustatic control on super sequences of the Zagros Mountains of Iran. *Tectonophysics* 451:56–70. DOI: https://doi.org/10.1016/j.tecto.2007.11.046.

Hontzsch S., Scheibner C., Brock J. P., Kuss J. (2013) Circum-Tethyan carbonate platform evolution during the Palaeogene: The Prebetic platform as a test for climatically controlled facies shifts. *Turkish Journal of Earth Sciences* 22:891–918. DOI: https://doi.org/10.3906/yer-1207-8.

James G. A., Wynd J. G. (1965) Stratigraphic nomenclature of Iranian oil consortium agreement area. *AAPG Bulletin* 49:2182–2245.

Jehangir Khan M., Ghazi S., Mehmood M., Yazdi A., Naseem A. A., Serwar U., Zaheer A., Ullah H. (2021) Sedimentological and provenance analysis of the Cretaceous Moro formation Rakhi Gorge, Eastern Sulaiman Range, Pakistan. *Iranian Journal of Earth Sciences* 13 (4): 252–266. DOI: https://doi.org/10.30495/ijes.2022.1917721.1564.

Joudaki M., Asnavandi H., Mahmoodi Panah F., Baghbani D. (2020) The regional facies analysis and depositional environments of the Oligocene and Lower Miocene deposits; Zagros Basin, SW of Iran. *Carbonates and Evaporites* 35 (2) DOI: https://doi.org/10.1007/s13146-020-00575-8.

Kakemem U., Adabi M. H., Sadeghi A., Kazemzadeh M. H. (2016) Biostratigraphy,paleoecology and paleoenvironmental reconstruction of the Asmari formation in Zagros basin, southwest Iran. *Arabian Journal of Geosciences* 9 (121) DOI: https://doi.org/10.1007/s12517-015-2152-5.

Kalanat B., Vaziri-Moghaddam H., Vahidinia M. (2014) Comparison of sequence stratigraphy and depositional environment of Asmari Formation in the Fars, Khuzestan and Lurestan areas of Zagros basin. *Scientific Semiannual Journal Sedimentary Facies* 7 (1): 107–124. DOI: https://doi.org/10.22067/sed.facies.v7i1.18648.

Kamalifar F., Aleali M., Ahmadi V., Mirzaiee A. (2020) Facies distribution, paleoenvironment and sequence stratigraphy model of the Oligo-Miocene Asmari Fm. (Fars Province, south of Iran). *Turkish Journal of Earth Sciences* 29:664–683.

Kershaw S., Brunton F. R. (1999) Paleozoic stromatoporoid taphonomy: Ecologic and environmental significance. *Palaeogeography, Palaeoclimatology, Palaeoecology* 14:313–328.

Khanali T., Seyrafian A. (2012) Biostratigraphy and microfacies of the Asmari formation in the Zagros Basin: Age and environmental correlation. *Petroleum Geology Journal of Iran* 3 (4): 38–51.

Khatibi mehr M., Adabi M. H., Mosavi tasuj M. R., Vaziri-Moghadam H., Sadeghi A. (2012) Microfacie, geochemistry and sedimentary environment of Jahrom formation in Kuh-e-Ghach, southeast Lar. *Petroleum Geology Journal of Iran* 26:97–118.

Langer M., Hottinger L. (2000) Biogeography of selected "larger" foraminifera. *Micropaleontology* 46:57–86.

Lees G. (1933) Reservoir rocks of Persian oil wells. *American Association of Petroleum Geologists Bulletin* 17:224–240.

Luciani V., Cobianchi M. (1999) The Bonarelli Level and other black shales in the Cenomanian – Turonian of the northeastern Dolomites (Italy): calcareous nannofossil and foraminiferal data. *Cretaceous Research* 20:135–167.

Martin-Martin M., Guerrera F., Tosquella J., Tramontana M. (2021) Middle Eocene carbonate platforms of the westernmost Tethys. *Sedimentary Geology* 415:105861. DOI: https://doi.org/10.1016/j.sedgeo.2021.105861.

——— (2020) Paleocene-Lower Eocene carbonate platforms of westernmost Tethys. *Sedimentary Geology* 404:105674. DOI: https://doi.org/10.1016/j.sedgeo.2020.105674.

Mirzaee Mahmoodabadi R. (2023) Assessment of evolution of the sedimentary environment of Paleocene-Eocene succession in Shiraz area based on sequence stratigraphic evidences. *Applied Sedimentology* 11 (21): 182–207. DOI: https://doi.org/10.22084/psj.2022.26615.1364.

Moallemi S. A., Adabi M. H., Sadeghi A. (2010) Depositional history of Jahrom formation based on distribution of benthic foraminifera and strontium isotope stratigraphy on the Bushehr area. *Scientific Quarterly Journal of Geosciences* 19 (74): 169–176. DOI: https://doi.org/10.22071/gsj.2010.57354.

Morsilli M., Bosellini F. R., Pomar L., Hallock P., Aurell M., Papazzoni C. A. (2012) Mesophotic coral buildups in a prodelta setting (Late Eocene, southern Pyrenees, Spain): a mixed carbonate–siliciclastic system. *Sedimentology* 59 (3): 766–794.

Motiei H. (1993) Stratigraphy of Zagros. 536. Tehran: Geological Survey of Iran Publication

Naseri-Karimvand F., Moussavi-Harami R., Mahboubi A., Ghabeishavi A., Shabafrooz R. (2019) Depositional environment and sequence stratigraphy of the Oligocene-Miocene deposits North and East of Dehdasht, Izeh Zone, Zagros Basin. *Iranian Journal of Earth Sciences* 30 (2): 143–166.

Nebelsick J. H., Stingl T. V., Rasser M. (2001) Autochthonous facies and Allochthonous debris flows compared: Early oligocene carbonate facies patterns of the lower Inn valley (Tyrol, Austria). *Facies* 44:31–46.

Parvaneh Nejad Shirazi M., Seddighi M., abadi P. Balicheh khorram (2020) Lithostratigraphy, microbiostratigraph and sedimentary environment of Jahrom formation in northwest of Shiraz (Chellehgah Sepidan). *Journal of Geoscience* 29 (116): 229–238. DOI: https://doi.org/10.22071/gsj.2019.163457.1588.

Payros A., Pujalte V., Tosquella J., Orue-Etxebarria X. (2010) The Eocene storm-dominated foralgal ramp of the western Pyrenees (Urbasa–Andia formation): An analogue of future shallow-marine carbonate systems. *Sedimentary Geology* 228 (3): 184–204. DOI: https://doi.org/10.1016/j.sedgeo.2010.04.010.

Rajabi M., Senemari S., Parvaneh Nejad Shirazi M., Bahrammaneshtehrani M. (2021) Biostratigraphy, Microfacies and palaeoecology of the Asmari formation in Makhmal Kuh section, Lurestan Province, western Iran. *Applied Sedimentology* 9 (17): 204–219. DOI: https://doi.org/10.22084/psj.2021.23429.1268.

Rasser M. W., Scheibner C., Mutti M. (2005) A paleoenvironmental standard section for Early Ilerdian tropical carbonate factories (Corbieres, France; Pyrenees, Spain). *Facies* 51:217–232.

Reading H. G. (1996) Sedimentary environments: Processes, facies and stratigraphy. 3rd Oxford, UK: Blackwell Science

Richardson R. K. (1924) The geology and oil measures of southwest Persia. *Journal of the Institute of Petroleum* 1:256–283.

Romero J., Caus E., Rosell J. (2002) A model for the palaeoenvironmental distribution of larger foraminifera based on late Middle Eocene deposits on the margin of the South Pyrenean basin (NE Spain). *Palaeogeography, Palaeoclimatology, Palaeoecology* 179 (1): 43–56.

Roozpeykar A., Moghaddam I. M. (2015) Biostratigraphy, facies analysis and paleoecology of the Asmari formation in the northwest of Behbahan, south-western Iran. *Carbonates Evaporites* 30:387–400. DOI: https://doi.org/10.1007/s13146-014-0225-2.

Saadat S., Ghoorchi M., Dabiri R. (2023) Extracting clay minerals with emphasis on Bentonite in Eastern Iran, using Landsat 8 and ASTER images. *Iranian Journal of Earth Sciences* 15 (3): 188–194. DOI: https://doi.org/10.30495/ijes.2023.1973739.1815.

Sadeghi R., Jokar M. (2018) Microbiostratigraphy of the Jahrom formation in Nimbashi section, West Estahban, Fars. *Journal of Stratigraphy and Sedimentology Researches* 34 (3): 73–94. DOI: https://doi.org/10.22108/jssr.2019.113070.1069.

Sahraeyan M., Bahrami M., Arzaghi S. (2014) Facies analysis and depositional environments of the OligoceneeMiocene Asmari Formation, Zagros Basin, Iran. *Geoscience Frontiers* 5:103–112. DOI: https://doi.org/10.1016/j.gsf.2013.03.005.

Scheibner C., Speijer R. (2008) Late Paleocene-Early Eocene Tethyan carbonate platform evolution - A response to long- and short-term paleoclimatic change. *Earth Science Reviews* 90:71–102. DOI: https://doi.org/10.1016/j.earscirev.2008.07.002.

Sepehr M., Cosgrove J. W. (2004) Structural Framework of the Zagros Fold-Thrust Belt, Iran. *Marine and Petroleum Geology* 21:829–843. DOI: https://doi.org/10.1016/j.marpetgeo.2003.07.006.

Serra-Kiel J., Hottinger L., Caus E., Drobne K., Ferrandez C., Jauhri A. K., Less G., et al. (1998) Larger foraminiferal biostratigraphy of the Tethyan Paleocene and Eocene. *Bulletin de la Société géologique de France* 169:281–299.

Seyrafian A., Vaziri-Moghadam H., Arzani N., Taheri A. (2011) Facies analysis of the asmari formation in central and North-Central Zagros Basin, Southwest Iran: Biostratigraphy, paleoecology and diagenesis. *Revista Mexicana de Ciencias Geolgicas* 28 (3): 439–458.

Shabafrooz R., Mahboubi A., Vaziri-Moghaddam H., Ghobeishavi A., Moussavi-Harami R. (2015) Depositional architecture and sequence stratigraphy of the Oligo– Miocene Asmari platform; Southeastern Izeh Zone, Zagros Basin, Iran. *Facies* 61:423. DOI: https://doi.org/10.1007/s,10347.014.0423.3.

Soltani Najafabadi M., Babazadeh S.A., Aleali M., Asgari Pirbaluti B. (2018) Microfacies and sedimentary environment of Jahrom Formation in Saldoran and Dasht- Zari sectione, Shahr-e-Kord, high Zagros. *Scientific Quarterly Journal of Geosciences* 27 (108): 115–124. DOI: https://doi.org/10.22071/gsj.2018.69267.

Stocklin J. (1968) Structural history and tectonics of Iran. *American Association of Petroleum Geologists Bulletin* 52:1229–1258. DOI: https://doi.org/10.1306/5D25C4A5-16C1-11D7-8645000102C1865D.

Thomas N.A. (1948) The Asmari Limestone of southwest Iran. *National Iranian Oil Company, Report 706*

Tosquella J., MartIn-MartIn M., Guerrera F., Serrano F., Tramontana M. (2022) Eocene carbonate platform of the central-western Malaguides (Internal Betic Zone, S Spain) and its meaning for the Cenozoic paleogeography of the westermost Tethys. *Palaeogeography, Palaeoclimatology, Palaeoecology* 589:110840. DOI: https://doi.org/10.1016/j.palaeo.2022.110840.

Van Buchem F. S. P., Allan T. L., Laursen G.V., Lotfpour M., Moallemi A., Monibi S., Motiei H., Pickard N. A. H., Tahmasbi A. R., VedreneVand B. (2010) Regional stratigraphic architecture and reservoir types of the Oligo.Miocene deposits in the Dezful Embayment (Asmari and Pabdeh formations) SW Iran. *Geological Society, London, Special Publications* 329:219–263.

Vaziri-Moghaddam H., Kimiagari M., Taheri A. (2006) Depositional environment and sequence stratigraphy of the Oligocene–Miocene Asmari Formation in SW Iran, Lali Area. *Facies* 52:41–51.

Vaziri-Moghaddam H., Seyrafian A., Taheri A., Motiei H. (2010) Oligocene–Miocene ramp system (Asmari Formation) in the NW of the Zagros basin, Iran: Microfacies, paleoenvironment and depositional sequence. *Revista Mexicana de Ciencias Geológicas* 27 (1): 56–71.

Wilson J. L. (1975) Carbonate Facies in Geologic History. 471. Berlin: Springer-Verlag

Yazdanpanah S. S., Ahmadi V., Arian M., maleki Z. (2022) Sedimentary environment and sequence stratigraphy of Jahrom Formation with a view on Paleo-ecology in the interior Fars, Zagros (SW Iran). *Journal of Environmental Science and Technology* 24 (9): 95–112. DOI: https://doi.org/10.30495/jest.2022.63297.5506.

Zulnoorian H., Mirbeik Sabzevari K., Asgari-Pirbalouti B., Shahrokhi S. V., Baharvand S. (2023) Biostratigraphy of the late Eocene-Miocene (Jahrom & Asmari Formations) in the west and southeast of the Shahr-e kord (Central Zagros). *Advanced Applied Geology* 13 (3): 641–660. DOI: https://doi.org/10.22055/aag.2022.41898.2318.